1521-0103/371/1/1–14$35.00
THE JOURNAL OF PHARMACOLOGY AND EXPERIMENTAL THERAPEUTICS
https://doi.org/10.1124/jpet.119.260281
J Pharmacol Exp Ther 371:1–14, October 2019

SEP-363856, a Novel Psychotropic Agent with a Unique, Non-D_2 Receptor Mechanism of Action[S]

Nina Dedic,[1] Philip G. Jones,[1] Seth C. Hopkins, Robert Lew, Liming Shao, John E. Campbell, Kerry L. Spear, Thomas H. Large, Una C. Campbell, Taleen Hanania, Emer Leahy, and Kenneth S. Koblan

Sunovion Pharmaceuticals, Marlborough, Massachusetts (N.D., P.G.J., S.C.H., R.L., L.S., J.E.C., K.L.S., T.H.L., U.C.C., K.S.K.); and PsychoGenics, Paramus, New Jersey (T.H., E.L.)

Received May 24, 2019; accepted July 10, 2019

ABSTRACT

For the past 50 years, the clinical efficacy of antipsychotic medications has relied on blockade of dopamine D_2 receptors. Drug development of non-D_2 compounds, seeking to avoid the limiting side effects of dopamine receptor blockade, has failed to date to yield new medicines for patients. In this work, we report the discovery of SEP-363856 (SEP-856), a novel psychotropic agent with a unique mechanism of action. SEP-856 was discovered in a medicinal chemistry effort utilizing a high throughput, high content, mouse-behavior phenotyping platform, in combination with in vitro screening, aimed at developing non-D_2 (anti-target) compounds that could nevertheless retain efficacy across multiple animal models sensitive to D_2-based pharmacological mechanisms. SEP-856 demonstrated broad efficacy in putative rodent models relating to aspects of schizophrenia, including phencyclidine (PCP)-induced hyperactivity, prepulse inhibition, and PCP-induced deficits in social interaction. In addition to its favorable pharmacokinetic properties, lack of D_2 receptor occupancy, and the absence of catalepsy, SEP-856's broad profile was further highlighted by its robust suppression of rapid eye movement sleep in rats. Although the mechanism of action has not been fully elucidated, in vitro and in vivo pharmacology data as well as slice and in vivo electrophysiology recordings suggest that agonism at both trace amine-associated receptor 1 and 5-HT_{1A} receptors is integral to its efficacy. Based on the preclinical data and its unique mechanism of action, SEP-856 is a promising new agent for the treatment of schizophrenia and represents a new pharmacological class expected to lack the side effects stemming from blockade of D_2 signaling.

SIGNIFICANCE STATEMENT

Since the discovery of chlorpromazine in the 1950s, the clinical efficacy of antipsychotic medications has relied on blockade of dopamine D_2 receptors, which is associated with substantial side effects and little to no efficacy in treating the negative and cognitive symptoms of schizophrenia. In this study, we describe the discovery and pharmacology of SEP-363856, a novel psychotropic agent that does not exert its antipsychotic-like effects through direct interaction with D_2 receptors. Although the mechanism of action has not been fully elucidated, our data suggest that agonism at both trace amine-associated receptor 1 and 5-HT_{1A} receptors is integral to its efficacy. Based on its unique profile in preclinical species, SEP-363856 represents a promising candidate for the treatment of schizophrenia and potentially other neuropsychiatric disorders.

Introduction

Schizophrenia is a chronic and disabling psychiatric disorder that affects approximately 1% of the global population. It is characterized by positive symptoms (e.g., hallucinations, delusions, and thought disorders), negative symptoms (e.g., flat affect, anhedonia, alogia, and avolition), and cognitive deficits (e.g., impaired memory, attention, and executive functioning). Despite advances in our understanding of the pathophysiology, schizophrenia remains one of the most challenging diseases to treat due to the diversity of clinical symptoms, the heterogeneity of clinical response, the side effects of current treatments, and its association with high morbidity and mortality (Insel, 2010; Meyer-Lindenberg, 2010; Girgis et al., 2019).

Antipsychotics have been the standard of care for schizophrenia since the discovery of chlorpromazine in the 1950s (Charpentier et al., 1952; Laborit et al., 1952; Lehmann and Ban, 1997). Since then, numerous new antipsychotics have been launched, but they have essentially the same mechanism of action, mediating their efficacy against the positive symptoms through antagonism of dopamine D_2 and/or serotonin 5-HT_{2A} receptors. Although improvements in drug safety have been made, a focus on the same molecular targets has

At the time these studies were conducted, all authors were employees of either Sunovion Pharmaceuticals or PsychoGenics. Some authors are inventors on patents related to the subject matter.
[1]N.D. and P.G.J. contributed equally to the work.
https://doi.org/10.1124/jpet.119.260281.
[S] This article has supplemental material available at jpet.aspetjournals.org.

ABBREVIATIONS: CNS, central nervous system; DRN, dorsal raphe nucleus; EEG, electroencephalogram; EPS, extrapyramidal symptoms; FST, forced swim test; KO, knockout; MOA, mechanism of action; PCP, phencyclidine; PPI, prepulse inhibition; REM, rapid eye movement; TAAR1, trace amine-associated receptor 1; Tb, body temperature; VTA, ventral tegmental area.

not led to improved efficacy (Lieberman et al., 2005; Girgis et al., 2019). In fact, the negative and cognitive symptoms remain largely untreated by currently available antipsychotics. Furthermore, approximately 30% of patients have treatment-resistant schizophrenia (Samara et al., 2016). The urgency for new treatments is therefore apparent.

More recently, drug development efforts have focused on molecular targets other than D_2 and 5-HT_{2A} receptors, including GlyT1, D_1, D_4, D_3, N-methyl-D-aspartate (NMDA), mGluR2/3, α-amino-3-hydroxy-5-methyl-4-isoxazolepropionic acid (AMPA), 5-HT_{2C}, nicotinic $\alpha7$, muscarinic M_1/M_4, H_3, NK-3, and σ receptors (Miyamoto et al., 2000; Karam et al., 2010; Girgis et al., 2019). However, despite promising efficacy in preclinical models for many of these targets, most novel, non-D_2/5-HT_{2A} mechanisms have shown limited or no success in clinical trials (Girgis et al., 2019). Thus, it is crucial to pursue alternative strategies for novel drug development for schizophrenia.

Traditional drug discovery efforts have been focused on designing compounds with high selectivity and potency for a target protein of interest. Unfortunately, in psychiatry there are few validated drug targets, in part due to the complexity of the disorders, rendering this approach largely unsuccessful. Phenotypic drug discovery does not require any knowledge of a molecular target(s) associated with a disease and has been associated with the discovery of first-in-class medications (Swinney and Anthony, 2011; Moffat et al., 2017). Examples include most anticonvulsants as well as antiviral drugs such as daclatasvir, which was discovered using a cell-based phenotypic screen (Belema and Meanwell, 2014). An in vivo phenotypic drug discovery approach could be particularly valuable for the discovery of new therapeutics for psychiatric indications that have a complex underlying pathophysiology and where polypharmacology is common and likely necessary for clinical efficacy. However, the selection of an appropriate target combination and the design of a safe and efficacious polypharmacological molecule are extremely difficult. We therefore took a target-agnostic in vivo approach by utilizing a mouse behavioral platform (Roberds et al., 2011; Alexandrov et al., 2015; Shao et al., 2016) together with anti-target in vitro screening to identify antipsychotic-like compounds that don't exert their effects through direct modulation of D_2 or 5-HT_{2A} receptors.

In this work, we report the discovery of SEP-363856 (SEP-856), a novel psychotropic agent with a unique, non-D_2/5-HT_{2A} mechanism of action. SEP-856 exhibits antipsychotic-like efficacy in vivo and demonstrates the potential for treating the positive and negative symptoms of schizophrenia. Although the mechanism of action has not been fully elucidated, in vitro and in vivo pharmacology data suggest that agonism at both trace amine-associated receptor 1 (TAAR1) and 5-HT_{1A} receptors is integral to its efficacy. The data presented in this work suggest that SEP-856 may have broad therapeutic efficacy in schizophrenia and potentially other psychiatric disorders.

Materials and Methods

Animals. Adult male C57BL/6J mice were utilized for behavioral screening, phencyclidine (PCP)-induced hyperactivity, catalepsy, and prepulse inhibition (PPI) studies, as well as patch–clamp recordings. The forced swim test (FST) was performed in adult male BalbC/J mice. Adult male Sprague-Dawley rats were utilized for electroencephalogram (EEG) recordings, microdialysis, in vivo cellular recordings, autoradiography, and PCP-induced deficits in social interaction. *In vivo* assessment of D_2 occupancy of SEP-856 was performed in nonhuman primate female baboons (*Papio anubis*). In vivo pharmacokinetic studies were performed in male adult ICR mice, adult male Sprague-Dawley rats, and male rhesus macaques (*Macaca mulatta*). Animals were maintained on a 12/12 light/dark cycle. The room temperature was maintained between 20°C and 23°C with a relative humidity maintained between 30% and 70%. Chow and water were provided ad libitum for the duration of the studies, unless otherwise stated. Animals were randomly assigned across treatment groups and studies conducted with experimenters blinded to the drug treatment. Further details (e.g., vendor, age, and/or weight range) are provided in the Supplemental Material.

All animal studies were conducted in accordance with the institutional animal care protocols complying with federal regulations and were approved by the respective Institutional Animal Care and Use Committees.

Test Compounds. Haloperidol, risperidone, quetiapine, clozapine, sertraline, PCP, 8-OH-DPAT, and WAY-100635 were purchased from Sigma-Aldrich. SEP-363856 [(*S*)-1-(4,7-dihydro-5*H*-thieno[2,3-*c*] pyran-7-yl)-*N*-methylmethanamine hydrochloride] and its enantiomer SEP-363855 were synthesized by Sunovion Pharmaceuticals, and all doses were corrected for salt content. Further information regarding formulation for each study is provided in the Supplemental Material.

Behavior-Based, Mouse Phenotypic Screening. The central nervous system (CNS) properties of SEP-856 were evaluated using the SmartCube® system, a high-throughput, automated mouse behavioral platform (Roberds et al., 2011; Alexandrov et al., 2015; Shao et al., 2016). Further experimental details are provided in the Supplemental Material.

Behavioral Phenotyping. Details on PPI, PCP-induced hyperactivity, catalepsy, FST, and PCP-induced deficits in social interaction are provided in the Supplemental Material.

EEG Recordings. EEG recordings were performed in seven adult male Sprague-Dawley rats using a crossover design. Animals were implanted with chronic recording devices for continuous recordings of electroencephalograph (EEG), electromyograph, core body temperature (Tb), and locomotor activity via telemetry (DQ ART 4.1 software; Data Sciences, St. Paul, MN). Following completion of the data collection, expert scorers determined states of sleep and wakefulness in 10-second epochs by examining the recordings visually using NeuroScore software (Data Sciences). All doses of SEP-856, caffeine, and vehicle were administered by oral gavage. A minimum of 3 days elapsed between doses. To evaluate the effects of SEP-856 on sleep/wake parameters during the inactive period, dosing occurred during the middle of the rats' normal inactive period. The first 6 hours of the recording were scored and analyzed. For additional details, please refer to the Supplemental Material.

In Vivo Microdialysis. Extracellular dopamine and serotonin levels were assessed in the prefrontal cortex and dorsal striatum using in vivo microdialysis in freely moving Sprague-Dawley rats. For detailed methods, please refer to the Supplemental Material.

In Vivo Pharmacokinetics Studies. Details on in vivo pharmacokinetic measurements are provided in the Supplemental Material.

In Vitro and In Vivo 5-HT_{1A} and D_2 Receptor Occupancy Studies. In vitro autoradiography was used to determine the effects of SEP-856 on [^{3}H]-8-OH-DPAT binding to 5-HT_{1A} receptors in rat brain sections. In vivo occupancy of SEP-856 at D_2 receptors was measured with [^{3}H]-raclopride in Sprague-Dawley rats and with [^{18}F]-fallypride–positron emission tomography in nonhuman primates (*Papio anubis*). For details, refer to Supplemental Material.

Patch–Clamp Recordings in the Dorsal Raphe Nucleus and Ventral Tegmental Area. In vitro whole–cell patch–clamp recording techniques were used in isolated slice preparations (male C57BL/6J mice, 4–16 weeks) of the dorsal raphe nucleus (DRN) and ventral tegmental area (VTA) to investigate the effects of SEP-856 on neuronal activity. The experiments examined the effects of SEP-856 (1–30 μM) on the activity of DRN and VTA neurons that were

characterized by their electrophysiological properties and/or their sensitivity to application of the 5-HT_{1A} receptor agonist 8-OH-DPAT (DPAT; 10 μM). Subsequently, effects mediated via the TAAR1 and/or via the 5-HT_{1A} receptor were investigated using the selective antagonist N-(3-Ethoxy-phenyl)-4-pyrrolidin-1-yl-3-trifluoromethyl-benzamide (EPPTB; 0.05–1 μM) and the selective antagonist WAY-100635 (WAY-635; 10 μM), respectively. All compounds were dissolved in either DMSO or ddH_2O and diluted with artificial cerebrospinal fluid (aCSF) to a final concentration from a minimum 1000-fold higher stock concentration (maximum slice DMSO concentration 0.1%). Whole–cell patch–clamp recordings were performed at room temperature using the blind version of the patch–clamp technique with either Axopatch 1D or Multiclamp 700B amplifiers. For detailed methods, refer to the Supplemental Material.

In Vivo Extracellular Single–Unit Recordings in the DRN. In vivo extracellular single–unit recordings were used to characterize the effects of SEP-856 on firing of DRN neurons in anesthetized, male Sprague-Dawley rats. Following surgery and insertion of the recording electrode, baseline firing activity of the neuron was recorded for at least 10 minutes prior to the compound administration. SEP-856 was tested at 1, 2, and 5 mg/kg by i.v. injection. After clear inhibitory effects were observed (3–5 minutes after compound administration), WAY-100635 (80 μg/kg, i.v.) was given to determine whether it could antagonize the inhibitory effect of SEP-856. Blood samples were taken 30 minutes following compound administration. For additional details, refer to the Supplemental Material.

In Vitro Pharmacology. The in vitro pharmacology of SEP-856 at known receptors and enzymes was assessed in broad panel screens (Eurofins CEREP SA, Celle-Lévescault, France; Ricerca, Taipei, Taiwan). For those targets at which SEP-856 (10 μM) demonstrated greater than 50% inhibition, dose–response curves were generated and inhibitory constant values were determined. Incubation conditions and additional details for equilibrium radioligand binding are listed in the Supplemental Material.

The functional (both agonist and antagonist) effects were also determined. Assays used to study the functional effects were as follows: Intracellular cAMP levels were determined for 5-HT_{1A}, 5-HT_7, TAAR1, and D_2, using either the DiscoveRx HitHunter cAMP XS^+ assay or the Cisbio Homogenous Time-Resolved Fluorescence (HTRF) cAMP assay. The 5-HT_{1A} was also studied using GTPγS binding. Impedance was used for 5-HT_{1B}, 5-HT_{1D}, and α_{2A}. Intracellular Ca^{2+} release was used for 5-HT_{2A} and 5-HT_{2C}. Inositol monophosphate (IP_1) accumulation was used for 5-HT_{2B}. D_2 was also studied using the DiscoveRx PathHunter β-arrestin recruitment assay.

Statistical Analyses. Statistical analyses were performed using the commercially available software GraphPad Prism v6.0, unless otherwise noted. Results are either presented as mean ± S.E.M. or mean ± S.D. (for pharmacokinetics (PK) analyses). Simple comparisons were evaluated with two-tailed, Student's t test. Multiple group comparisons were assessed with one-way ANOVA, followed by appropriate post hoc analyses. Time-dependent measures were assessed with repeated measures ANOVA followed by appropriate post hoc analyses. Statistical significance was defined as $P < 0.05$.

Results

SEP-856 Exhibits Antipsychotic-Like Activity in the Smartcube System. SEP-856 (Fig. 1A) was identified during a medicinal chemistry program designed to develop structurally and mechanistically novel antipsychotics using in vivo mouse phenotypic screening in combination with comprehensive in vitro and in vivo molecular profiling.

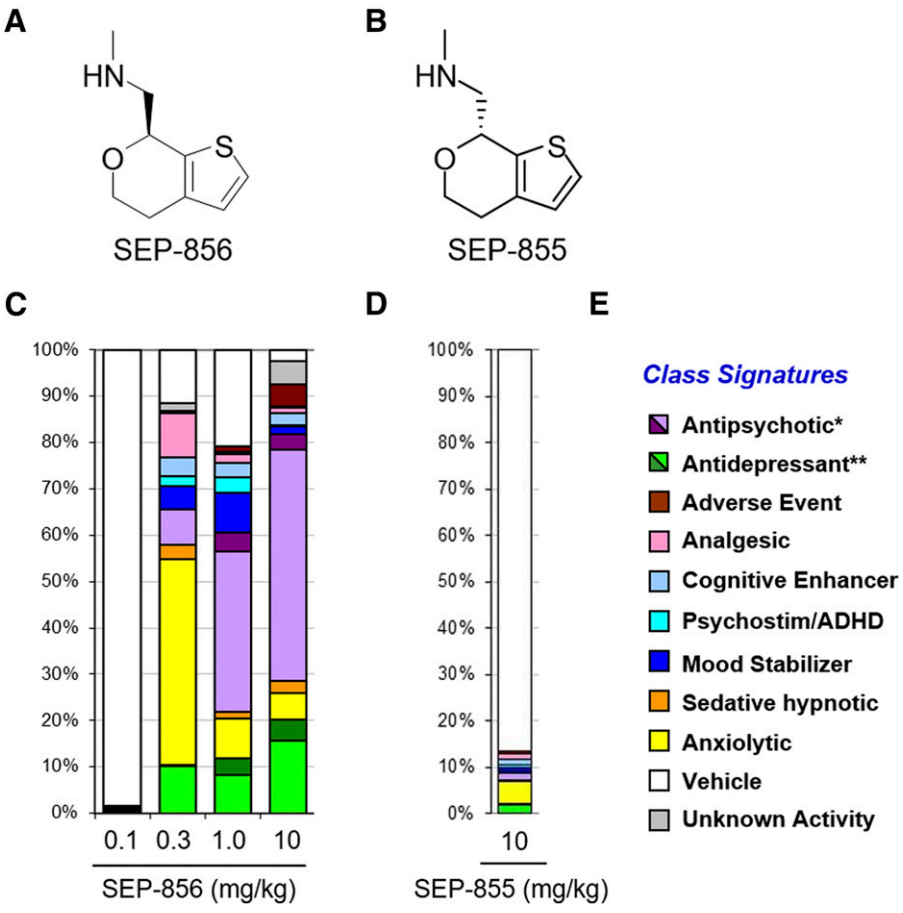

Fig. 1. SEP-856 exhibits a predominantly antipsychotic-like signature in SmartCube®. The chemical structures of SEP-856 (A) and its enantiomer SEP-855 (B). The behavioral signature of SEP-856 (C) includes anxiolytic (yellow) and antipsychotic (purple) components. In contrast, its enantiomer SEP-855 is largely behaviorally inactive in mice, represented by the vehicle-like white bar (D). The behavioral platform was established and validated with marketed CNS drugs, producing a library of drug-class signatures. (E) Each of the 15 classes is represented by a different color, as indicated [*antipsychotic (purple) and high-dose antipsychotic (dark purple); **antidepressant (green) and *high-dose antidepressant (dark green)]. N = 8–10 mice/group.

Screening was conducted during a 45-minute automated test session, in which mice were exposed to multiple challenges, and different behavioral domains were captured and analyzed using proprietary computer vision software and machine learning algorithms (Roberds et al., 2011; Alexandrov et al., 2015; Shao et al., 2016). The behavioral platform was established and validated with marketed CNS drugs, producing a library of drug-class signatures. Each class is represented by a different color; for example, purple and yellow indicate antipsychotic- and anxiolytic-like activity, respectively (Fig. 1E), and the behavioral activity is shown as a scale of 0% to 100%. The data in Fig. 1C demonstrated that SEP-856 was behaviorally active at three of four doses tested (0.3, 1, and 10 mg/kg, i.p.). At 0.3 mg/kg, SEP-856 was classified as an anxiolytic (represented by the primarily yellow color of the column) but showed a dose-dependent increase in an antipsychotic classification (purple), such that the signatures at 1 and 10 mg/kg were predominantly antipsychotic-like. As a comparison, the signatures of marketed antipsychotic drugs are shown in Supplemental Fig. 1. In addition, SEP-856 showed a modest antidepressant-like signal, illustrated by the green signal at 0.3, 1, and 10 mg/kg. Overall, the results indicate that SEP-856 is CNS active and exhibits a behavioral signature similar to known antipsychotic drugs. Interestingly, its enantiomer, SEP-363855 (SEP-855), showed little behavioral activity at 10 mg/kg (i.p.), a dose at which SEP-856 was fully efficacious (Fig. 1, B and D).

In Vitro Pharmacology. To investigate the molecular targets mediating the response to SEP-856, the compound was tested against several panels of known molecular targets (ion channels, G protein-coupled receptors (GPCRs), and enzymes; Supplemental Tables 1–4). At 10 μM, SEP-856 showed >50% inhibition of specific binding at α_{2A}, α_{2B}, D_2, 5-HT_{1A}, 5-HT_{1B}, 5-HT_{1D}, 5-HT_{2A}, 5-HT_{2B}, 5-HT_{2C}, and 5-HT_7 receptors. Inhibitory constant values are shown in Table 1 ranging from 0.031 to 21 μM. No significant activity of SEP-856 was observed at any of the enzymes studied (up to a concentration of 100 μM).

Receptor panel screening and follow-up functional testing showed that SEP-856 exhibited a range of activities at several receptors (Table 2). The most notable activity of SEP-856 was agonism at the human TAAR1 receptor (EC_{50} of 0.14 ± 0.062 μM, maximum efficacy (E_{max}) = 101.3% ± 1.3%) and the 5-HT_{1A} receptor (EC_{50} = 2.3 μM with values ranging from 0.1 to 3 μM, E_{max} = 74.7% ± 19.6%; Fig. 2B). Interestingly, activity at the human TAAR1 receptor demonstrated stereoselectivity in that SEP-855 (an enantiomer of SEP-856), which was inactive in the behavioral screening platform at 10 mg/kg (i.p.), had an EC_{50} of 1.7 μM (Fig. 2A). In D_2 receptor functional assays, SEP-856 exhibited weak partial agonism with EC_{50} values of 10.44 ± 4 μM (cAMP, E_{max} = 23.9% ± 7.6%; Fig. 2C) and 8 μM (β-arrestin recruitment, E_{max} = 27.1%). At 100 μM, 34% ± 1.16% inhibition was seen in the cAMP assay, and no antagonism was seen at concentrations up to 100 μM in the β-arrestin recruitment assay. Low potency partial agonist activities were also observed at 5-HT_{1B} (EC_{50} = 15.6 ± 11.6 μM, E_{max} = 22.4% ± 10.9%), 5-HT_{1D} (EC_{50} = 0.262 ± 0.09 μM, E_{max} = 57.1% ± 6.0%), and 5-HT_7 receptors (EC_{50} = 6.7 ± 1.32 μM, E_{max} = 41.0% ± 9.5%). In a functional assay of 5-HT_{2B} activity, SEP-856 showed no agonism up to a concentration of 100 μM, whereas norfenfluramine, the positive control, was a full agonist with an EC_{50} value of 0.140 μM. Little to no activity was detected at the 5-HT_{2A} receptor, with 29.3% agonism seen only at the highest tested concentration of 10 μM.

SEP-856 Exhibits High Brain Penetrance and Good Systemic Bioavailability Following Oral Administration. Behavioral phenotypic screening demonstrated that SEP-856 is CNS active in mice following 0.3, 1, and 10 mg/kg intraperitoneal administration. Consequently, the pharmacokinetics of SEP-856 in plasma was characterized in ICR mice, Sprague-Dawley rats, and rhesus macaques following oral and/or i.v. dosing. Biologic samples were collected over 8 or 24 hours postdose. Brain exposure was also assessed in mice and rats following *per os* (p.o.) administration. SEP-856 was rapidly absorbed, with maximum plasma and brain concentrations reached within 0.25–0.5 hours in mice and rats and maximum plasma concentrations reached within 6 ± 2.83 hours in monkeys (Supplemental Table 5). SEP-856 penetrated mouse and rat brains after oral administration (10 mg/kg), with average brain-to-plasma area under the curve ratios of approximately3-4 (Supplemental Fig. 2). In addition, SEP-856 plasma and brain levels were still detectable at 8 hours postdose with fairly consistent brain/plasma ratios over time. SEP-856's brain penetration and elimination pharmacokinetics as indicated by t_{max} and half life were similar to the plasma pharmacokinetics (Supplemental Table 5).

Oral bioavailability of SEP-856, determined by plasma area under the curve ratio after crossover oral and intravenous administrations, was high in rat and monkey with 58% to 120% and ~71%, respectively. Total plasma clearance of SEP-856 was relatively high in rat (5 mg/kg, i.v.) and monkey (5 mg/kg, i.v.) with 1.54 and 0.797 l/h per kilogram, respectively, and elimination half-lives of 1.2 and 3.1 hours, respectively.

SEP-856 Demonstrates Antipsychotic-Like Efficacy in Rodents. To demonstrate the antipsychotic-like profile of SEP-856, we performed a series of additional pharmacological studies that assess endophenotypes of schizophrenia and antidepressant efficacy in rodents.

Acute treatment with phencyclidine (PCP), which induces robust hyperactivity in rodents and psychosis-like symptoms in humans, is considered a valuable assay in preclinical research and is widely used to screen novel compounds for antipsychotic efficacy (Ratajczak et al., 2013; Steeds

TABLE 1

Receptor affinities.

Panel screens of up to 105 radioligand-binding assays and 34 enzyme assays were performed, and the affinity of SEP-856 was determined for receptors at which >50% inhibition was seen at 10 μM. Details of radioligands, incubation conditions , and the targets in the screening panels are listed in the Supplemental Material. Data are shown as mean ± S.E.M. ($n \geq 3$, $n = 1$ for 5-HT_{2B}).

Receptor	K_i (μM)
D_{2s}	21.3 ± 8.2
5-HT_{1A}	0.284 ± 0.056
5-HT_{1B}	1.90 ± 1.72
5-HT_{1D}	1.13 ± 0.21
5-HT_{2A}	17.25 ± 4.0
5-HT_{2B}	1.1
5-HT_{2C}	2.45 ± 0.82
5-HT_7	0.031 ± 0.003
α_{2A}	0.59 ± 0.06
α_{2B}	1.9 ± 0.10

TABLE 2

In vitro functional profile of SEP-856.

The functional effects of SEP-856 were determined for receptors at which >50% inhibition was seen in the panel screens. The in vitro pharmacology studies were run in both agonist and antagonist modes. The specific assays are listed in Materials and Methods. Data are shown as mean ± S.E.M. ($n \geq 3$).

Receptor	Agonist		Antagonist	
	EC_{50} (μM)	% E_{max}	IC_{50} (μM)	% Inhibition
TAAR1	0.140 ± 0.062	101.3 ± 1.3	NE	NE
5-HT_{1A}	2.3 ± 1.40	74.7 ± 19.6	NE	NE
5-HT_{1B}	15.6 ± 11.60	22.4 ± 10.9	NE	NE
5-HT_{1D}	0.262 ± 0.09	57.1 ± 6.0	NE	NE
5-HT_{2A}	>10	29.3 @ 10 μM	NE	NE
5-HT_{2C}	30 ± 4.5	63.3 ± 3.1	NE	NE
5-HT_7	6.7 ± 1.32	41.0 ± 9.5	NE	NE
α_{2A}	>10	39.4 ± 4.2	NE	NE
α_{2B}	NE	NE	NE	NE
D_{2L} (cAMP)	10.44 ± 4.0	23.9 @ 10 μM	>100	34.0 ± 1.16
D_{2L} (arrestin recruitment)	8.02	27.1 @ 10 μM	>100	<25 @ 100 μM

NE, no effect (<30% @ 30 μM).

et al., 2015; Moffat et al., 2017). Single oral administration of SEP-856 (0.3, 1, and 3 mg/kg; 30-minute pretreatment time) resulted in a dose-dependent inhibition of PCP-induced hyperactivity responses in C57BL/6J mice (one-way ANOVA $F_{(5, 59)} = 18.96$, $P < 0.0001$; Tukey's post hoc test, $P < 0.05$) with an ED_{50} of approximately 0.3 mg/kg (Fig. 3A). The positive control, clozapine, also significantly reduced PCP-induced hyperactivity. Small but significant decreases in baseline activity were observed with SEP-856 at the highest dose of 3 mg/kg (one-way ANOVA $F_{(5, 59)} = 5.5$, $P < 0.001$; Tukey's post hoc test, $P < 0.05$; Supplemental Fig. 3A).

Another behavioral assay that is routinely used to identify novel antipsychotic agents is PPI of the acoustic startle response (Geyer et al., 2001). PPI occurs when a startle-eliciting stimulus (i.e., the pulse) is preceded by a stimulus of lower intensity (i.e., the prepulse) and the amplitude of the startle response is reduced. Single oral administration of SEP-856 (0.3, 1, 3, 10, and 30 mg/kg; 30-minute pretreatment time) in C57BL/6J mice resulted in

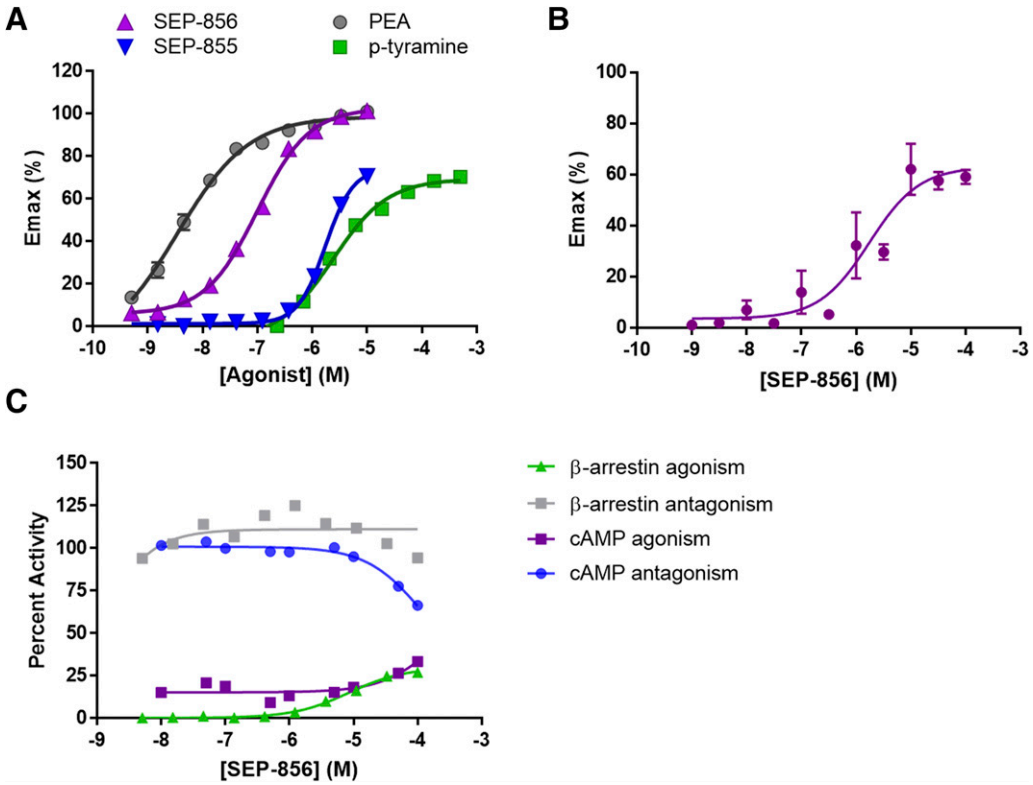

Fig. 2. Functional effects of SEP-856 at TAAR1, 5-HT_{1A}, and D_2 receptors. The functional effects of SEP-856 were determined using HEK-293 cells expressing TAAR1 (A), 5-HT_{1A} (B), or D_2 (C) receptors. cAMP accumulation was determined for TAAR1 using the DiscoveRx HitHunter cAMP assay. The inactive enantiomer of SEP-856 (SEP-855) was also tested along with the trace amines phenethylamine (PEA) and p-tyramine. Inhibition of forskolin-stimulated cAMP levels was used for the 5-HT_{1A} ($n = 4$) and D_2 receptors; cAMP levels were determined with the DiscoveRx HitHunter cAMP XS^+ assay or the Cisbio HTRF, cAMP assay. The D_2 receptor was also studied using the PathHunter β-arrestin recruitment assay. Representative traces are shown for (A and C).

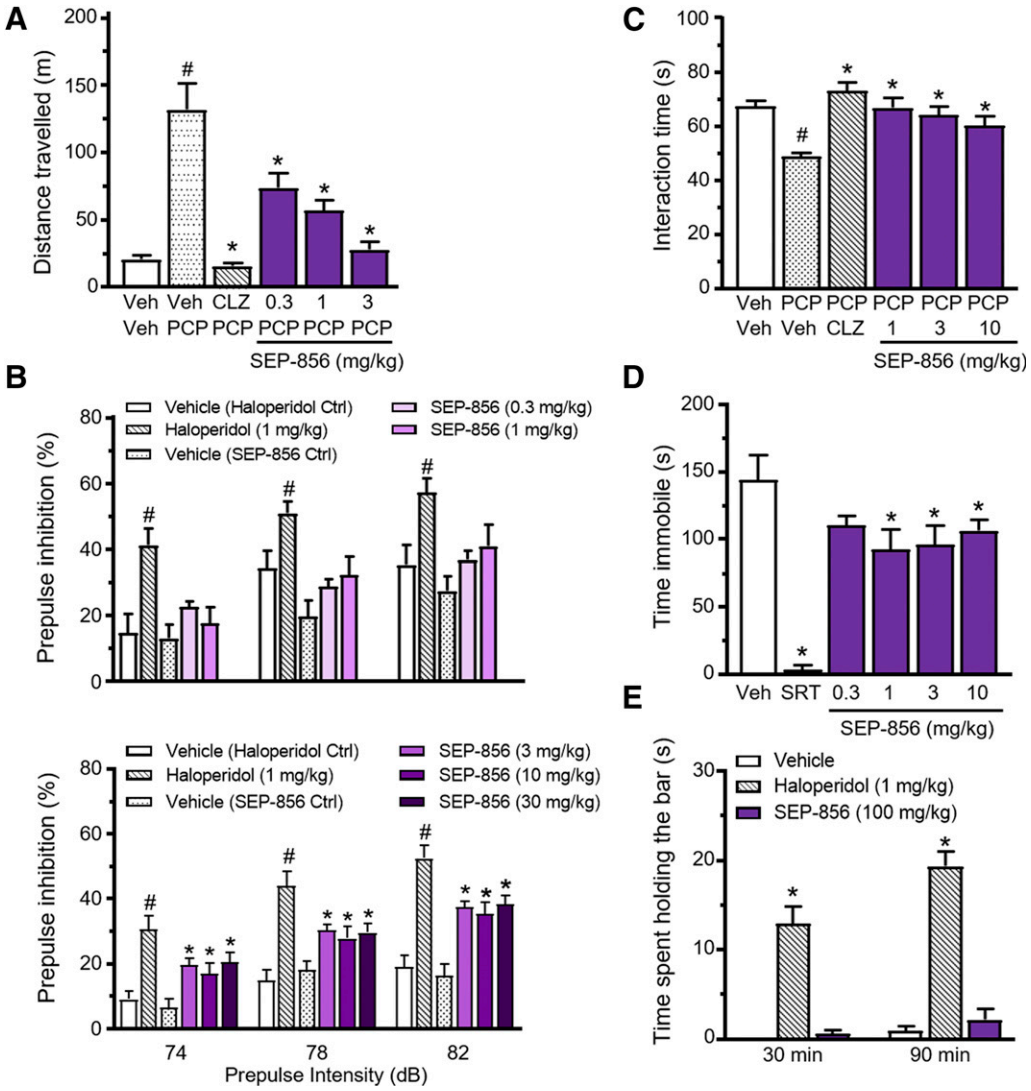

Fig. 3. SEP-856 demonstrates antipsychotic- and antidepressant-like activity without inducing catalepsy. (A) Oral SEP-856 administration dose-dependently reduced PCP-induced hyperactivity in C57BL/6J mice (one-way ANOVA + Tukey's post hoc test, $^{*}P < 0.05$ vs. Veh/PCP, $^{\#}P < 0.05$ vs. Veh/Veh). Clozapine and PCP were dosed at 1 and 5 mg/kg i.p., respectively. (B) PPI measured in C57BL/6J mice was significantly increased by haloperidol (i.p.) and SEP-856 at 3, 10, and 30 mg/kg (p.o.) compared with their respective vehicle controls (10% DMSO for haloperidol and 20% cyclodextrin for SEP-856; one-way ANOVA + Tukey's post hoc test, $^{*\#}P < 0.05$). (C) Social interaction deficits induced by subchronic PCP treatment (2.5 mg/kg, s.c., twice daily for 5 days) in Sprague-Dawley rats were significantly attenuated by acute clozapine (2.5 mg/kg, i.p.) and SEP-856 (p.o.) treatment at all doses tested (one-way ANOVA + Tukey's post hoc test, $^{*}P < 0.05$ vs. PCP/Veh, $^{\#}P < 0.05$ vs. Veh/Veh). (D) Acute sertraline (20 mg/kg, i.p.) and 1, 3, and 10 mg/kg SEP-856 (p.o.) dosing reduced immobility time in the FST in Balb/CJ mice compared with vehicle controls (one-way ANOVA + Tukey's post hoc test, $^{*}P < 0.05$ vs. Veh). (E) In contrast to haloperidol (i.p.), acute SEP-856 (p.o.) treatment did not induce catalepsy in the mouse (C57BL/6J) bar test, as seen by the lack of increase in time spent holding the bar compared with vehicle (two-way ANOVA + Tukey's post hoc, $^{*}P < 0.05$ vs. Veh). CLZ, clozapine; SRT, sertraline. N = 8–12/group. Data are shown as mean ± S.E.M.

a dose-dependent increase in PPI compared with the respective vehicle treatment (Fig. 3B), with significant increases observed at 3, 10, and 30 mg/kg (two-way ANOVA: treatment effect $F_{(3, 102)} = 19.9, P < 0.0001$; db effect $F_{(2, 102)} = 30.97, P < 0.0001$; Dunnett's post hoc test, $P < 0.05$). Unlike the positive control haloperidol, SEP-856 improved PPI at dose levels that had no confounding effects on baseline startle responses (Supplemental Fig. 3B).

In contrast to positive symptoms, negative symptoms of schizophrenia, including anhedonia, blunted affect, and social withdrawal, are more difficult to model in animals (Jones et al., 2011; Wilson et al., 2015). However, subchronic treatment with PCP reliably produces social interaction deficits in rodents that may mimic certain aspects of negative symptoms such as social withdrawal (Steeds et al., 2015). Sprague-Dawley rats were subcutaneously injected with PCP (2 mg/kg) or vehicle twice daily for 5 consecutive days, followed by behavioral assessment on day 6. The PCP-induced deficit in social interaction was significantly attenuated by single oral administration of SEP-856 at 1, 3, and 10 mg/kg (one-way ANOVA $F_{(5, 56)} = 8.33, P < 0.0001$; Tukey's post hoc test, $P < 0.05$). The positive control, clozapine (2.5 mg/kg, i.p.), also showed efficacy that was comparable to SEP-856 (Fig. 3C). This suggests that SEP-856 may have potential benefits against some of the negative symptoms of schizophrenia, such as social withdrawal.

The effects of SEP-856 (0.3, 1, 3, and 10 mg/kg) were additionally evaluated in the mouse FST, a behavioral assay

that is acutely sensitive to all major classes of marketed antidepressants drugs (Porsolt et al., 1977). Single oral administration of SEP-856 significantly reduced immobility time at 1, 3, and 10 mg/kg compared with vehicle (one-way ANOVA $F_{(5, 44)} = 13.24$, $P < 0.0001$; Tukey's post hoc test, $P < 0.05$; Fig. 3D), suggesting that SEP-856 may also exhibit antidepressant-like activity. However, no clear dose-dependent effect was observed, and the magnitude of response was smaller than that produced by the positive control sertraline (20 mg/kg, i.p.).

One of the issues associated with antipsychotic drugs is the potential to develop extrapyramidal symptoms (EPS), which can be assessed in mice by measuring the induction of catalepsy using the bar test. Oral administration of SEP-856 (100 mg/kg) produced no effects in the bar test, whereas haloperidol (1 mg/kg, i.p.) significantly increased the amount of time mice spent holding the bar at 30- and 90-minute postdosing (two-way ANOVA: treatment effect $F_{(2, 54)} = 107.7$, $P < 0.0001$; time effect $F_{(1, 54)} = 9.4$, $P < 0.005$; Dunnet's post hoc test, $P < 0.05$). Importantly, these data indicate that SEP-856 was not associated with cataleptic effects at doses at least 30-fold higher than efficacious dose levels in mice (Fig. 3E).

The plasma and brain exposures to SEP-856 in the mouse PCP-induced hyperactivity and PPI tests as well as the rat subchronic PCP-induced social interaction test are shown in Supplemental Table 6. Taken together, our results indicate a clear antipsychotic-like profile of SEP-856 in rodents and corroborate the initial findings obtained in the behavioral screening platform.

SEP-856 Decreases Rapid Eye Movement Sleep. The activation of 5-HT_{1A} and TAAR1 has been shown to promote a generalized increase in wakefulness, increased latency to sleep, and suppression of rapid eye movement (REM) sleep (Revel et al., 2012b; Black et al., 2017; Schwartz et al., 2017). Because SEP-856 exhibits agonism at and TAAR1 and 5-HT_{1A}, we investigated whether it affects sleep architecture, as determined by telemetric recordings of the EEG, electromyogram, Tb, and locomotor activity in Sprague-Dawley rats. SEP-856 and the positive control caffeine were administered during the middle of the light (inactive) period, followed by 6 hours of recordings. Oral SEP-856 administration (1, 3, and 10 mg/kg) produced a dose-dependent decrease in REM sleep, increase in latency to REM sleep, and increase in cumulative wake time (Fig. 4, A and B; Supplemental Fig. 4). SEP-856 had no effect on the cumulative non-REM time and latency to non-REM (Supplemental Fig. 4). The differential effect on REM was further evident by a dose-dependent decrease in the REM: non-REM ratio (Fig. 4C). Caffeine promoted wakefulness, as expected, with additional characteristic increases in locomotion and Tb that SEP-856 did not produce (Supplemental Fig. 4). Collectively, these results suggest that SEP-856 promotes vigilance when given during the light (inactive) phase.

SEP-856 Interacts with Central 5-HT_{1A} but Not D_2 Receptors. In addition to TAAR1, in vitro testing revealed that SEP-856 exhibits agonist activity at 5-HT_{1A} and D_2 receptors . Consequently, we conducted a series of experiments to determine whether SEP-856 interacts with these two targets in vivo.

First, receptor autoradiography was used to assess SEP-856 occupancy at D_2 receptors in the rat brain using the radioligand [^{3}H]-raclopride. SEP-856 (10 mg/kg, i.p.) or vehicle was administered to Sprague-Dawley rats, followed by administration of [^{3}H]-raclopride (60 μCi/kg, i.v.) 30 minutes later. D_2 receptor occupancy was assessed at 60 minutes post–SEP-856 (or vehicle) administration in coronal sections of the striatum (region of interest) and cerebellum (reference region). Despite high plasma (~1300 ng/ml), brain (~7900 ng/g), and CSF (~1800 ng/ml) exposures, SEP-856 resulted in 12.6% ± 6.4% receptor occupancy at D_2 (Supplemental Table 7), which was not statistically different from vehicle controls (two-tailed t test, $P = 0.27$). For comparison, activity in the rat PCP-induced social interaction deficit assay (1–10 mg/kg) and mouse PCP-induced hyperactivity test (0.3–3 mg/kg) was seen at much lower exposures (Supplemental Table 6). Thus, acute administration of SEP-856 did not produce significant occupancy at D_2 receptors in the rat brain at plasma concentrations up to 200-fold greater than those that were behaviorally efficacious.

We additionally conducted in vivo positron emission tomography imaging to determine whether SEP-856 also fails to occupy D_2 receptors in the nonhuman primate brain. Imaging

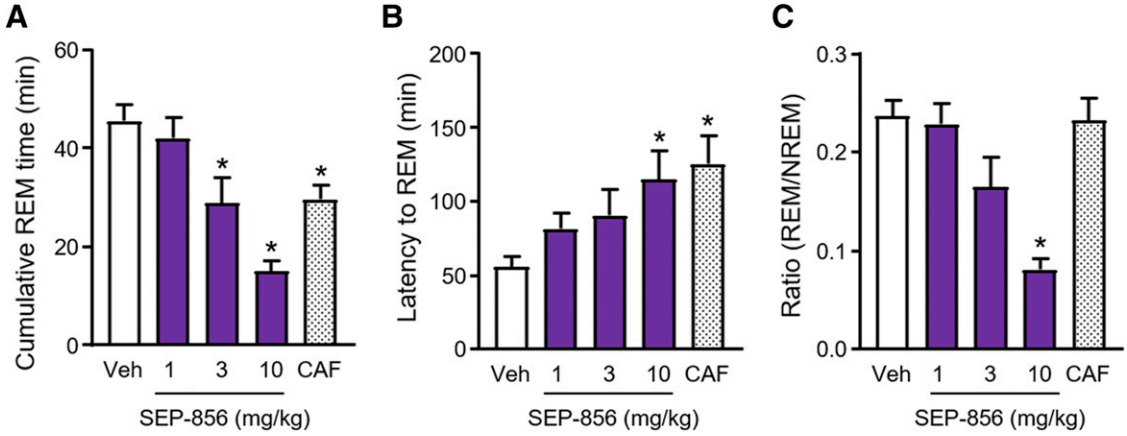

Fig. 4. SEP-856 decreases REM sleep in rats. (A) Acute, oral administration of SEP-856 led to a dose-dependent reduction in cumulative REM sleep (A), increase in latency to REM (B), and a decrease in REM/non-REM ratio (C) in Sprague-Dawley rats over the 6-hour recording period (one-way repeated-measures ANOVA + two-tailed t test, *$P < 0.05$ vs. Veh). Dosing occurred in the middle of the inactive phase, at the beginning of Zeitgeber time 7. The positive control caffeine (10 mg/kg, p.o. CAF) produced similar effects on REM time and latency without altering the REM/non-REM ratio. Additional parameters are presented in Supplemental Fig. 4. $N = 7$. Data are shown as mean ± S.E.M.

was conducted in two anesthetized baboons using the radiotracer [^{18}F]-fallypride. The percent occupancy was evaluated using a blockade protocol comparing [^{18}F]-fallypride regional binding potential at baseline and following SEP-856 administration (~7.25 mg/kg, i.v. 30 minutes prior to [^{18}F]-fallypride injection). Venous blood samples were taken before and at various time points after SEP-856 administration. SEP-856 showed D_2 receptor occupancy levels of 9.1% ± 3.3%, 6.2% ± 6.1%, and 9.6% ± 8.8% in the caudate, putamen, and globus pallidus, respectively (Fig. 5; Supplemental Table 8). Similar to the observations in rats, SEP-856 did not produce significant occupancy at D_2 receptors despite achieving high plasma concentrations (i.e., 2850 ± 250 ng/ml at 60 minutes and 1765 ± 125 ng/ml at 180 minutes after SEP-856 administration). Importantly, this finding demonstrates that the antipsychotic-like behavioral profile of SEP-856 is independent of direct D_2 receptor modulation.

Next, we used in vitro autoradiography to evaluate the effects of SEP-856 on [^{3}H]-8-OH-DPAT (a 5-HT$_{1A}$ agonist radioligand) binding to 5-HT$_{1A}$ receptors in the rat brain. Slide-mounted rat brain sections were incubated with 2 nM [^{3}H]-8-OH-DPAT in the presence and absence of SEP-856 (0.1, 1, and 10 μM). Nonspecific binding was defined by 10 μM 5-HT. SEP-856 produced a concentration-dependent displacement of [^{3}H]-8-OH-DPAT binding in all regions evaluated (Supplemental Fig. 5). Given the similar degree of [^{3}H]-8-OH-DPAT binding in all brain areas, IC_{50} values for SEP-856 displacement of [^{3}H]-8-OH-DPAT binding were only determined for the septum and motor/somatosensory cortex (referred to as cortex). SEP-856 displaced [^{3}H]-8-OH-DPAT in a concentration-dependent manner, with a mean IC_{50} of 619 and 791 nM in the cortex and septum, respectively (Fig. 6). These results demonstrate that SEP-856 can bind to central 5-HT$_{1A}$ receptor sites in vitro.

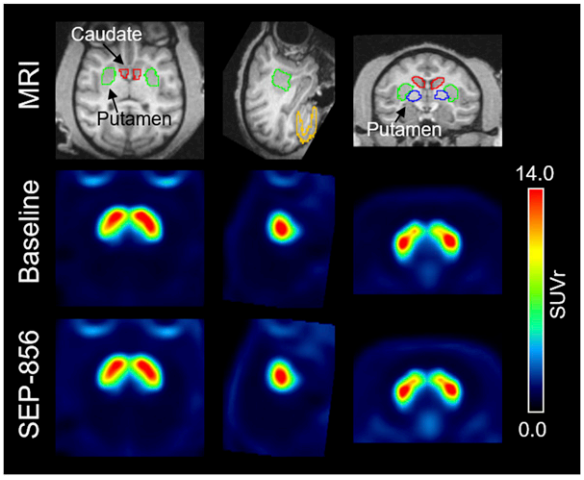

Fig. 5. SEP-856 does not exhibit significant occupancy at D_2 receptors in nonhuman primates. Representative magnetic resonance (for anatomic reference) and mean summed positron emission tomography images, before and after administration of SEP-856, are shown from top to bottom for one animal. Axial, sagittal, and coronal slices are shown from left to right. Regions of interest, including the caudate, putamen, and globus pallidus, were manually outlined. Average [^{18}F]fallypride positron emission tomography images over 180 minutes of acquisition are presented at baseline and following bolus i.v. administration of SEP-856 (7.25 mg/kg). The occupancy was estimated using the BP_{ND}-derived Simplified Reference Tissue Model. SUVr, relative standardized uptake value.

SEP-856 Inhibits Neuronal Firing in the DRN and VTA In Vitro. To investigate the effect of SEP-856 on neuronal activity and obtain further insights into its mechanism of action, we performed whole–cell patch–clamp recordings in isolated slice preparations of the DRN and the VTA of C57BL/6J mice. The DRN and VTA express a high abundance of 5-HT$_{1A}$ and TAAR1 receptors, respectively (Lindemann et al., 2008; Celada et al., 2013; Christian and Berry, 2018). After the determination of repeatable responses, administration of SEP-856 was repeated in the presence of the selective TAAR1 antagonist EPPTB and/or the selective 5-HT$_{1A}$ receptor antagonist WAY-100635.

Whole–cell current–clamp recordings were made from 29 neurons within the DRN with a mean resting membrane potential of −46.1 ± 1.0 mV and a mean input resistance of 849 ± 61 MΩ. Based on changes in membrane potential and firing rates, 16 of the DRN neurons were characterized as being sensitive to the 5-HT$_{1A}$ agonist 8-OH-DPAT (DPAT), and 13 were classified as DPAT-insensitive (Supplemental Fig. 6). Based on their initial threshold activity, 44% (7 of 16) of DPAT-sensitive neurons were characterized as spontaneously active (discharging action potentials) and 56% (9 of 16) were quiescent. SEP-856 (10 μM) induced significant membrane hyperpolarization in eight of nine quiescent neurons (45.5 ± 1.9 to −49.0 ± 2.2 mV, post–SEP-856 washout to 46.1 ± 1.9 mV; paired two-tailed t test, $t_7 = 4.3$, $P = 0.004$; Fig. 7A). In contrast, one single neuron was depolarized by 2.1 mV. SEP-856 also significantly reduced the activity of five of seven spontaneously active DRN neurons (0.31 ± 0.10 Hz to 0.11 ± 0.04, post–SEP-856 washout to 0.20 ± 0.06 Hz; 69% ± 9.7% reduction; paired two-tailed t test, $t_4 = 3.2$, $P = 0.03$; Fig. 7A), whereas the remaining two neurons were largely unaffected. Collectively, administration of 10 μM SEP-856 induced an inhibitory response, determined by either a membrane hyperpolarization or a reduction in spontaneous firing rate, in 81% (13 of 16) of DPAT-sensitive neurons. In contrast, SEP-856 only induced an inhibitory response in 15% (2 of 13) of DPAT-insensitive neurons (Supplemental Fig. 6).

Next, the effects of 10 μM SEP-856 were examined in the presence of the 5-HT$_{1A}$ antagonist WAY-100635 (1 μM) in five DPAT-sensitive DRN neurons, two of which were spontaneously active and three of which were quiescent. In three of the five neurons, a membrane hyperpolarization of 1.9 ± 0.4 mV induced by SEP-856 was markedly reduced to 0.4 ± 0.1 mV when SEP-856 was reapplied in the presence of WAY-100635 (79% reduction; Fig. 7B; Supplemental Fig. 6). Similarly, the inhibitory effect of SEP-856 was almost completely blocked in a further neuron in the presence of WAY-100635, with the spontaneous firing rate being reduced by 47% (0.21–0.11 Hz) during control SEP-856 administration compared with just a 2% reduction (0.83–0.82 Hz) when SEP-856 was applied in the presence of WAY-100635 (Fig. 7B). In the remaining neuron, a 2.4 mV hyperpolarization induced by SEP-856 was slightly increased to 2.6 mV in the presence of WAY-100635. Thus, the inhibitory response induced by SEP-856 was reduced in the presence of the 5-HT$_{1A}$ antagonist WAY-100635, in the majority (4 of 5, 80%) of DRN neurons analyzed.

In addition, the effects of SEP-856 were examined in the presence of EPPTB in six DPAT-sensitive DRN neurons, three of which were spontaneously firing action potentials and three of which were quiescent. Overall, the inhibitory response induced by SEP-856 was unaffected in the presence of the

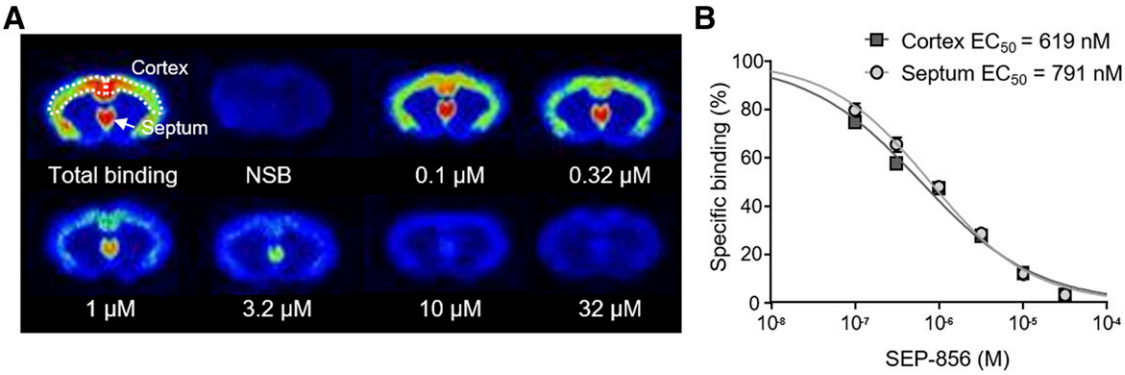

Fig. 6. SEP-856 binds to 5-HT_{1A} receptors in rat brain slices. (A) Autoradiographs of coronal brain sections depicting binding of the 5-HT_{1A} agonist [^{3}H]-8-OH-DPAT. The highest receptor binding was observed in the septum and throughout the cortex (illustrated by increasing intensity in yellow to red colors). (B) SEP-856 displaced [^{3}H]-8-OH-DPAT in a concentration-dependent manner, with an IC_{50} of 619 and 791 nM in the cortex and septum, respectively (n = 4 brains, two sections/brain). Sections were incubated with 2 nM [^{3}H]-8-OH-DPAT and 10 μM serotonin for nonspecific binding (NSB), 0.1% DMSO for total binding, or SEP-856 (0.1–32 μM). Data are shown as mean ± S.E.M.

TAAR1 antagonist EPPTB, in the majority (5 of 6, 83%) of DRN neurons tested (Fig. 7C).

Following the assessment of SEP-856 effects on DRN neuronal firing, whole–cell patch–clamp recordings were also made from 23 neurons within the VTA (mean resting membrane potential of −40.7 ± 0.7 mV and a mean input resistance of 935 ± 104 MΩ) (Supplemental Fig. 7). All of these neurons were spontaneously active once whole–cell configuration had been established with a mean firing rate of 1.97 ± 0.60 Hz, although activity did not persist in all cases. SEP-856 induced an inhibitory response in approximately half of the recorded VTA neurons (Fig. 7D; Supplemental Fig. 7). This response was characterized by a significant hyperpolarization of 2.8 ± 0.5 mV in 42% (8 of 19) of the neurons (−42.6 ± 1.3 to −45.3 ± 1.4 mV; paired two-tailed t test, $t_7 = 5.8$, $P = 0.0007$) and a significant reduction in spontaneous firing rate in 55% (11 of 20) of the neurons (from 0.6 ± 0.18 to 0.18 ± 0.07 Hz; 71.4% ± 7% reduction; paired two-tailed t test, $t_{10} = 3.3$, $P < 0.008$; Fig. 7D).

Interestingly, recordings from two neurons showed that the inhibitory response of SEP-856 (1 μM) was reduced in the presence of 1 μM EPPTB (Fig. 7F), but persisted in the presence of the 5-HT_{1A} antagonist WAY-100635 (Fig. 7E). However, observations from additional neurons are necessary to further validate the ability of EPPTB to attenuate the inhibitory effect of SEP-856 in the VTA.

Overall, SEP-856 induced significant inhibitory responses in DPAT-sensitive neurons of the DRN and a subset of VTA neurons. In contrast to the inhibitory effects of SEP-856 in the DRN, which were primarily mediated via activation of 5-HT_{1A} receptors, the response in the VTA appeared to be at least partially mediated via the activation of TAAR1.

SEP-856 Inhibits DRN Neuronal Firing In Vivo. The observation that SEP-856's inhibitory effects in the DRN were mediated by 5-HT_{1A} led us to additionally investigate DRN neuronal firing in vivo by recording extracellular single–unit activities in anesthetized Sprague-Dawley rats. In accordance with previous work (Martin et al., 1999), application of 8-OH-DPAT inhibited DRN firing, which was subsequently reversed by 0.08 mg/kg WAY-100635 (Supplemental Fig. 8). SEP-856 (2 mg/kg, i.v.) significantly decreased DRN neuron discharges to 87% of the baseline rate (from 9.83 ± 1.4 to 1.4 ± 0.33 spikes/10 seconds; two-tailed t test, $t_2 = 5.9$, $P < 0.03$) during the initial 10 minutes postdosing (Fig. 8, A and B). Thirty minutes after SEP-856 administration, the inhibitory effect was no longer detectable and firing rates were restored to baseline levels. SEP-856 plasma exposures determined 30 minutes postdosing were 422 ± 22.5 ng/ml. When SEP-856 was tested at a higher dose (5 mg/kg, i.v.), firing activity was completely suppressed and the inhibition was fully reversed by intravenous administration of 0.08 mg/kg WAY-100635 (Fig. 8, C and D). Similarly, the inhibitory effect of 2 mg/kg SEP-856 was also reversed by WAY-100635 (Supplemental Fig. 8). These results support the earlier in vitro finding in mice, and further suggest that part of SEP-856's mechanism of action is characterized by suppression of serotonergic neuronal firing via activation of 5-HT_{1A} autoreceptors.

SEP-856 Does Not Alter Dopamine and Serotonin Release in the Striatum or Prefrontal Cortex. To determine whether the inhibitory action of SEP-856 in DRN neurons translates into changes in synaptic serotonin levels, we measured 5-HT release in vivo using microdialysis in freely-moving rats. Although SEP-856 demonstrated no occupancy at D_2 receptors in vivo, its antipsychotic-like behavioral profile, TAAR1 activity, and ability to inhibit VTA neurons suggest potential modulation of dopaminergic circuits independent of direct dopamine receptor regulation. We therefore also assessed dopamine release. Changes in monoamine levels were monitored over a 240-minute period following oral administration of vehicle, 3, 10, or 30 mg/kg SEP-856. Interestingly, no significant changes in extracellular levels of dopamine or 5-HT were observed in striatum or prefrontal cortex following SEP-856 administration (Supplemental Fig. 9).

Antipsychotic-Like Effects of SEP-856 Are Partially Mediated by 5-HT_{1A} Receptors. Although the microdialysis findings revealed no changes in SEP-856–mediated 5-HT release, the in vitro pharmacology results as well as the slice and in vivo electrophysiology data suggest that agonism at 5-HT_{1A} receptors is integral to SEP-856's mechanism of action in both mice and rats. Consequently, we evaluated whether the 5-HT_{1A} receptor antagonist WAY-100635 would attenuate the inhibitory behavioral effects of SEP-856 in the mouse PCP-induced hyperactivity test. C57BL/6J mice were injected with

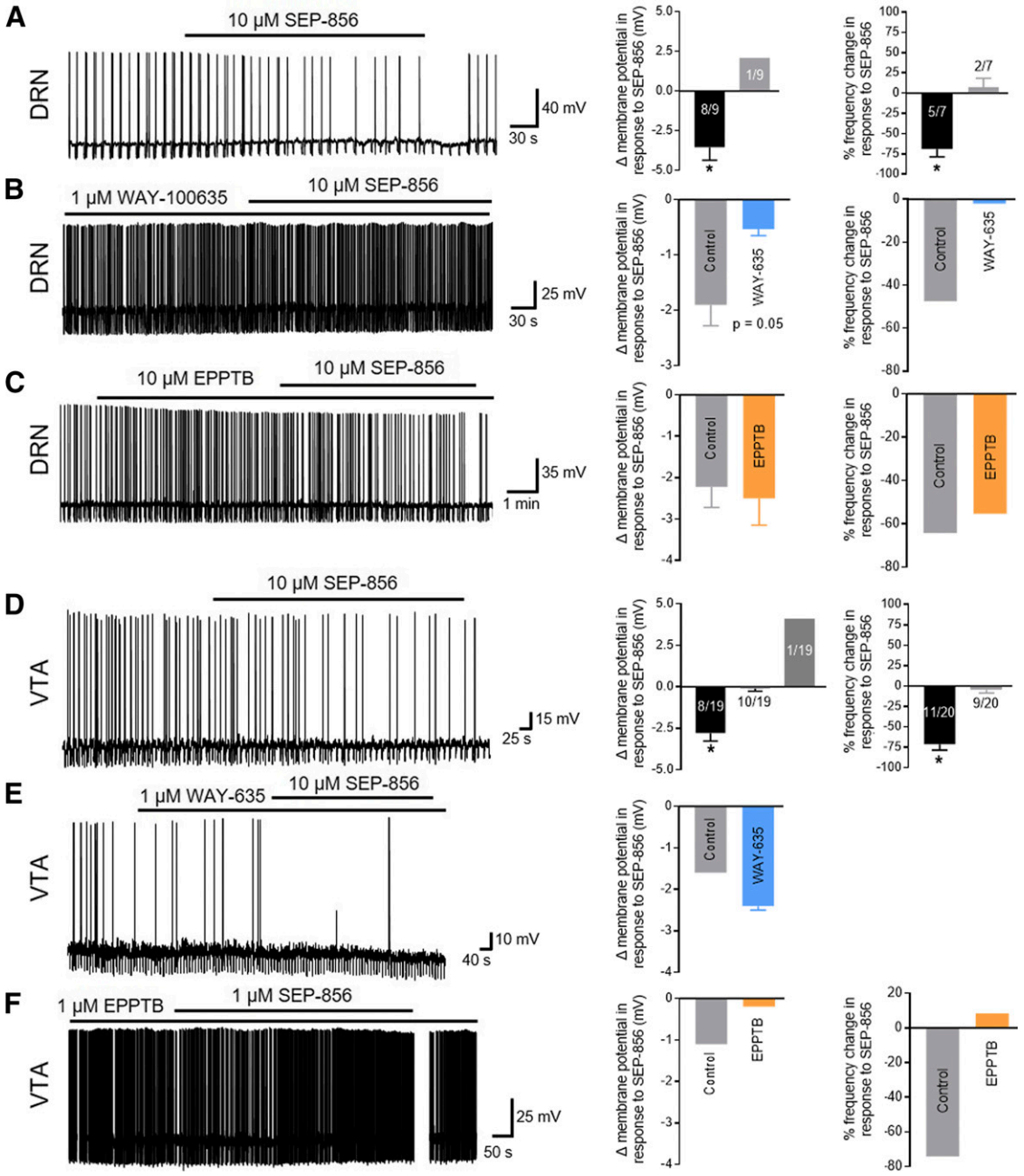

Fig. 7. SEP-856 inhibits firing of DRN and VTA neurons in vitro. Representative whole–cell patch–clamp recordings from DRN and VTA brain slices of C57BL/6J mice are shown on the left, and quantification histograms on the right. Compound-induced effects were determined based on significant changes in membrane potential (millivolts) and/or firing rate (Hertz) and expressed relative to baseline (Δ membrane potential and % frequency change). DRN neurons were classified as sensitive or insensitive to the 5-HT_{1A} agonist 8-OH-DAPT. (A) SEP-856 induced inhibitory responses in the majority of spontaneously active, 8-OH-DAPT–sensitive DRN neurons. This inhibitory effect was absent in four of five neurons in the presence of the 5-HT_{1A} antagonist WAY-100635 (B) but persisted in five of six neurons in the presence of the TAAR1 antagonist EPPTB (C). (D) Based on significant changes in membrane potential and/or firing rate, approximately half of the spontaneously-active neurons in the VTA were inhibited by SEP-856 treatment when compared with baseline. This effect persisted in presence of WAY-100635 (E, $n = 2$ neurons) but was reduced in the presence of EPPTB (F, $n = 2$ neurons). Histograms show neuronal responses following administration of SEP-856 alone (control, A and D) and in the presence of WAY-100635 (B and E) or EPPTB (C and F). Solid horizontal bars indicate the time frame of compound administration to the slice. Two-tailed t test, $^*P < 0.05$. Abbreviations: WAY-100635 (WAY or WAY-635). Data are shown as mean ± S.E.M.

WAY-100635 (1 mg/kg, i.p.) or saline (i.p.) 10 minutes prior to SEP-856 dosing (3 mg/kg, oral), followed by PCP administration (5 mg/kg, i.p.) 30 minutes later. Consistent with our previous findings, single oral administration of SEP-856 significantly inhibited PCP-induced hyperactivity responses (Fig. 8E). Pretreatment with WAY-100635 partially attenuated the inhibitory effects of SEP-856 on the total distance traveled (one-way ANOVA $F_{(5,\ 51)} = 22.11$, $P < 0.0001$; Tukey's post hoc test, $P < 0.05$). Taken together, the results indicate that the antipsychotic-like effects of SEP-856 in the PCP-induced hyperactivity test may be partially mediated through 5-HT_{1A} receptors.

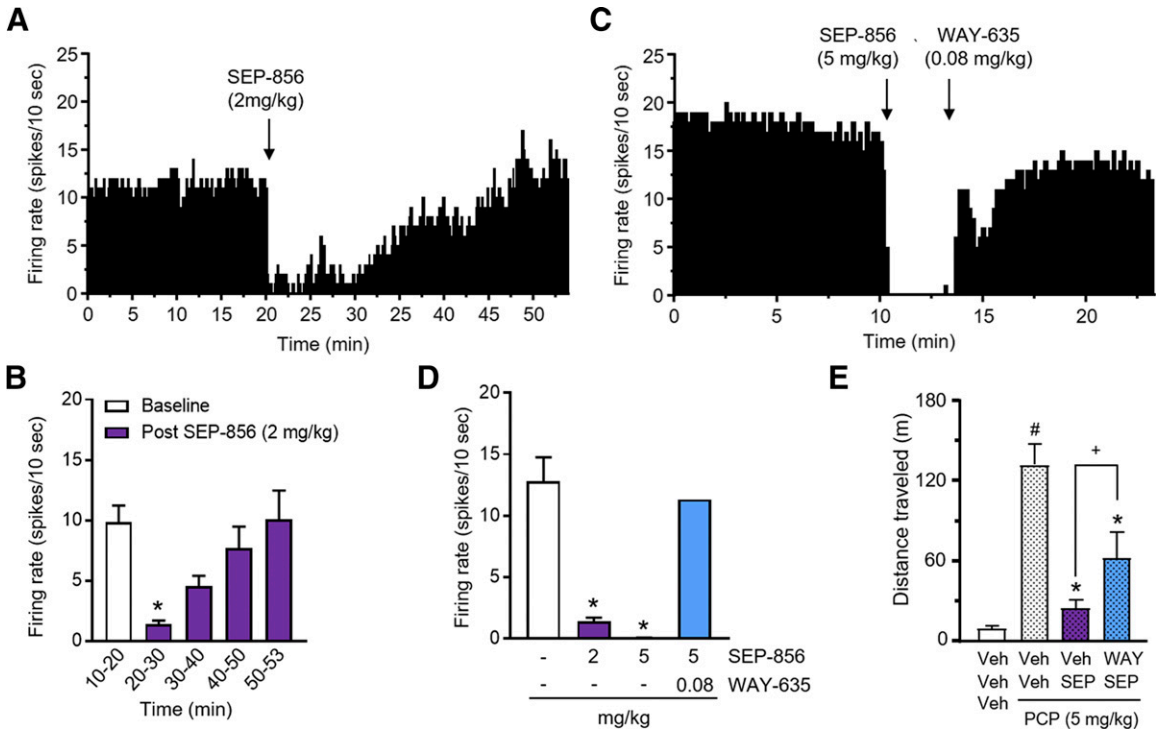

Fig. 8. SEP-856 inhibits firing of DRN in vivo and partially attenuates PCP-induced hyperactivity through 5-HT_{1A} receptors. (A) SEP-856 (2 mg/kg, i.v.) decreased single-unit discharges of DRN neurons in anesthetized Sprague-Dawley rats ($n = 2$). (B) The most significant inhibition was observed during the first 10 minutes after dosing, with discharge rates returned to baseline levels ~20 minutes later (48–53 minutes after start of recording). (C and D) Neuronal DRN firing rates were completely suppressed by a higher dose of SEP-856 (5 mg/kg, i.v., two-tailed t test, $^*P < 0.05$, $n = 2$), and this inhibition was subsequently reversed by WAY-100635 (0.08 mg/kg; $n = 1$). (E) Pretreatment of WAY-100635 (1 mg/kg, i.p.) partially attenuated the ability of SEP-856 (3 mg/kg, p.o.) to reduce PCP-induced hyperactivity in C57BL/6J mice (one-way ANOVA + Tukey's post hoc test, $^+P < 0.05$, $^*P < 0.05$ vs. Veh/Veh/PCP, $^\#P < 0.05$ vs. Veh/Veh/Veh; $n = 9$ to 10/group). Abbreviations: WAY-100635 (WAY or WAY-635). Data are shown as mean ± S.E.M.

Discussion

Numerous advances have been made in understanding the potential role of receptors other than D_2 in contributing to drug efficacy and specific side effects in schizophrenia. Recent antipsychotic drug development has focused on non-D_2 targets, including D_1, D_4, D_3, NMDA, 5-HT_{2A}, 5-HT_{2C}, M_1, M_4, H_3, NK_3, and σ receptors (Miyamoto et al., 2005; Karam et al., 2010; Girgis et al., 2019). However, to date, no compound lacking D_2 receptor blockade has proven effective for any symptom dimension of schizophrenia. Although several non-D_2 mechanisms, including mGlu2/3 receptor agonism and GlyT1 inhibition, have demonstrated efficacy in nonclinical and clinical proof-of-concept studies, positive results in Phase III clinical trials are still lacking (Marsman et al., 2013; Kinon et al., 2015; Girgis et al., 2019). In this study, we used an in vivo mouse phenotypic screening platform in combination with comprehensive in vitro and in vivo profiling to identify compounds that exhibited behavioral similarity to known antipsychotics but do not act through D_2 or 5-HT_{2A} mechanisms. This led to the discovery of SEP-856, a compound that showed potent antipsychotic-like properties without inducing catalepsy. In addition, SEP-856 demonstrated potential antidepressant-like effects, suppressed REM sleep, and modulated firing in a subset of VTA and DRN neurons.

To decipher the molecular mechanism of action (MOA) of SEP-856, its effects were initially studied in panel screens of large numbers of receptors, ion channels, and enzymes. Subsequent studies identified activity at TAAR1, 5-HT_{1A}, 5-HT_{1D}, α_{2A}, and D_2 receptors. Weak partial agonism of D_2 receptors (EC_{50} = 8–10 μM, E_{max} 24%–27%), and some very low-potency antagonism (34% inhibition at 100 μM), was seen in in vitro assays. It should be noted that this antagonism was assay dependent as, for instance, no antagonist response was seen in the β-arrestin recruitment assay. Despite this in vitro activity, additional experiments indicated that the MOA of SEP-856 does not include in vivo blockade at D_2 given the lack of receptor occupancy in rat and monkey seen at doses/exposures that are efficacious in rodent behavioral assays. Furthermore, the demonstrated central occupancy of 5-HT_{1A} receptors, as well as the partial reversal of PCP-induced hyperactivity in the presence of WAY-100635, indicates that 5-HT_{1A} agonism contributes to the MOA of SEP-856. This was further supported by SEP-856's ability to induce significant inhibitory responses via 5-HT_{1A} receptors in putative serotonergic neurons in the DRN in vitro and in vivo. Notably, the inhibitory response induced in a subset of VTA neurons was mediated, at least in part, via activation of TAAR1, suggesting that SEP-856 modulates firing of putative serotonergic and dopaminergic neurons through distinct mechanisms.

TAAR1 is a GPCR activated by trace amines and expressed in multiple regions of the mammalian brain, including the limbic system, DRN and VTA (Borowsky et al., 2001; Burchett and Hicks, 2006; Lindemann et al., 2008; Rutigliano et al., 2018). Recent studies have extensively characterized TAAR1 functions, elucidating its important role in modulating dopaminergic circuitry and its potential implications in neuropsychiatric disorders (Borowsky et al., 2001; Leo et al., 2014;

Gainetdinov et al., 2018; Schwartz et al., 2018). Revel et al. (2011) reported the first selective TAAR1 agonist (RO5166017) and demonstrated its inhibitory effects on the firing of dopaminergic and serotonergic neurons. In addition, the antipsychotic-like profile of full and partial TAAR1-selective agonists was shown by their ability to inhibit cocaine and PCP-induced hyperlocomotion in rodents despite their lack of affinity for D_2 receptors (Revel *et al.*, 2011, 2012b, 2013). Similarly, SEP-856 was able to block PCP-induced hyperactivity without significantly occupying D_2 receptors. Unfortunately, the lack of suitable TAAR1 antagonists prevented direct assessment ofTAAR1's contribution to the antipsychotic-like activity of SEP-856 in vivo.

TAAR1's ability to regulate presynaptic dopaminergic neurotransmission makes it an interesting target for a number of psychiatric disorders (Lindemann et al., 2008; Revel et al., 2011; Leo et al., 2014). Along these lines, TAAR1 agonists have demonstrated efficacy in genetic mouse models of hyperdopaminergia, including DAT knockout (KO) mice and rats (Revel et al., 2011, 2012a,b). The observed effects on dopaminergic signaling presumably occur via functional physical interaction of TAAR1 with D_2 receptors and potentially also with the dopamine transporter (Espinoza et al., 2011; Leo et al., 2014; Harmeier et al., 2015; Leo and Espinoza, 2016). Cell culture studies have shown that TAAR1 is normally located intracellularly but can translocate to the plasma membrane when coexpressed with D_2 receptors (Espinoza et al., 2011; Harmeier et al., 2015). The ability of TAAR1 to modulate dopaminergic tone was also demonstrated in TAAR1 KO mice. Under baseline conditions, striatal dopamine release was not altered in KO animals compared with wild-type controls but was augmented following an amphetamine challenge (Wolinsky et al., 2007; Lindemann et al., 2008). Follow-up work by Leo et al. (2014), using microdialysis and fast-scan cyclic voltammetry, revealed increased levels of dopamine specifically in the nucleus accumbens but not in the dorsal striatum of TAAR1 KO mice (Lindemann et al., 2008). In accordance, TAAR1 agonists have been reported to suppress VTA neuronal firing (Revel et al., 2011) and inhibit electrically-evoked dopamine release (Leo et al., 2014). SEP-856 exerted inhibitory effects in VTA neurons, which were likely mediated via activation of TAAR1. Interestingly, the inhibitory response was only observed in half of the recorded cells, pointing to a selective suppression of a subset of VTA neurons by SEP-856. The lack of D_2 occupancy, in addition to the inhibitory effects on VTA neuronal firing, potentially suggests modulation of presynaptic dopamine dysfunction by SEP-856. Abnormalities in dopamine synthesis capacity, baseline synaptic dopamine levels, and dopamine release have been reported in schizophrenia patients, and are not targeted by current antipsychotic treatments (Howes et al., 2012; Jauhar et al., 2017; Kim et al., 2017; McCutcheon et al., 2018). Although SEP-856 demonstrated clear inhibitory effects on DRN and VTA neurons, it did not alter dopamine or 5-HT release in the striatum or prefrontal cortex. This could be due to a number of reasons, including the difficulty in detecting potential decreases in neurotransmitter release under baseline conditions using conventional microdialysis. Differential effects of SEP-856 on dopamine and/or serotonin release might primarily be detectable under stimulated conditions (e.g., following electrical, pharmacological, or behavioral challenges) or in a disease context (e.g., hyperdopaminergic state). In contrast, changes in dopaminergic and serotonergic cell firing do not necessarily translate into changes in dopamine/5-HT release (Berke, 2018). For example, dopamine release can be locally controlled by the presynaptic terminals themselves and thus show spatiotemporal patterns independent of cell body spiking (Floresco et al., 1998; Jones et al., 2010; Berke, 2018). In addition, SEP-856 might affect tonic versus phasic dopaminergic firing differentially, which could ultimately result in marked behavioral effects without necessarily altering overall dopamine levels. Additional experiments, applying both microdialysis and fast-scan cyclic voltammetry, will help to further elucidate the effect of SEP-856 on neurotransmitter release and firing kinetics under baseline and stimulated conditions.

In addition to TAAR1-mediated activity, 5-HT_{1A} agonism was identified as an integral part of the MOA of SEP-856. The 5-HT_{1A} receptor is highly expressed in the DRN, cortex, and limbic forebrain areas (e.g., hippocampus and amygdala), with lower densities detected in the basal ganglia, thalamus, substantia nigra, and VTA (Kia et al., 1996; Ito et al., 1999; De Almeida and Mengod, 2008). In the DRN, 5-HT_{1A} receptors are primarily somatodendritic autoreceptors that function to inhibit neuronal firing. In contrast, they are present as postsynaptic receptors in the hippocampus and amygdala (Celada et al., 2013). Thus, it will be interesting to test whether SEP-856 also acts in an inhibitory fashion in forebrain regions such as the hippocampus or prefrontal cortex.

The serotonergic circuitry has repeatedly been implicated in the pathophysiology of schizophrenia, in part due to the antipsychotic properties of 5-HT_{2A} antagonists (although primarily in combination with D_2 blockers). In addition, 5-HT_{2C} antagonists and compounds that target both receptors 5-HT_{2A}/5-HT_{2C} (e.g., ritanserin, vabicaserin, mianserin, SR46349B, etc.) have demonstrated some efficacy in schizophrenia (Girgis et al., 2019). Although evidence exists for the therapeutic efficacy of 5-HT_{1A} agonists in depression and anxiety, less is known about the potential contribution of these receptors to schizophrenia. Postmortem (Burnet et al., 1996, 1997; Simpson et al., 1996; Sumiyoshi et al., 1996) and neuroimaging studies (Kasper et al., 2002; Tauscher et al., 2002) have revealed alterations in 5-HT_{1A} receptor density in the cortex and amygdala of schizophrenic patients (Yasuno et al., 2004). Evidence in rodent models indicates that the activation of 5-HT_{1A} receptors prevents EPS induced by D_2 receptor blockade, modulates dopaminergic neurotransmission in the frontal cortex, positively influences mood, and attenuates NMDA receptor antagonist-induced cognitive and social interaction deficits (Newman-Tancredi, 2010; Celada et al., 2013). In addition, a number of compounds that combine partial agonism at 5-HT_{1A} receptors with antagonism (or partial agonism) at D_2 receptors (e.g., aripiprazole, perospirone, lurasidone, cariprazine, PF-217830, F-97013-GD, F-15063, and bifeprunox) appear to provide therapeutic benefits against a broader range of schizophrenia symptoms (Newman-Tancredi, 2010; Celada et al., 2013).

Interestingly, earlier work demonstrated that modulation of TAAR1 activity via the selective agonist RO5166017 increases the potency of 5-HT_{1A} partial agonists and alters the desensitization rate at the 5-HT_{1A} autoreceptors in the DRN

(Revel et al., 2011). This can occur by direct interaction of TAAR1 and 5-HT_{1A}, or by favoring interactions with the GPCR desensitization machinery. Consequently, Revel et al. (2011) proposed that cotreatment with a TAAR1 agonist might improve therapeutic efficacy of classic antidepressants, providing further support for compounds with dual 5-HT_{1A}/TAAR1 activity in the treatment of psychosis and mood. Notably, TAAR1 agonists and many antidepressants (especially those with 5-HT_{1A} activity) exert REM sleep suppression, which is not observed for most D_2-based antipsychotics (Tribl et al., 2013; Wichniak et al., 2017; Goonawardena et al., 2019). Thus, the robust REM suppression observed with SEP-856 could result from synergistic action on TAAR1 and 5-HT_{1A} receptors. However, agonism at TAAR1 and 5-HT_{1A} receptors might only partially contribute to SEP-856's MOA, with other (possibly not yet identified) targets likely playing key roles as well.

Although this work made use of multiple pharmacological rodent models and assays, it is important to mention that no animal model is, or ever will be, truly reflective of the underlying disease etiology of schizophrenia. Nevertheless, certain models serve as important investigational tools and are useful in the development of novel treatments, especially when the goals for a specific model and/or approach are clearly defined (Nestler and Hyman, 2010). Our goal was to identify a novel MOA for the treatment of schizophrenia by focusing on a desired clinical outcome—the combination of antipsychotic efficacy and lack of D_2-mediated side effects (e.g., EPS and endocrine effects). Ultimately, proof-of-concept studies in humans are required to determine whether preclinical findings will translate into therapeutic efficacy. SEP-856 is currently being evaluated for the treatment of schizophrenia in randomized, controlled clinical trials.

In summary, the approach used in this work represents an alternative to target-driven drug discovery as it relied on in vivo phenotypic and in in vitro (anti-target) screening, followed by subsequent verification in putative animal models of schizophrenia. Accordingly, the MOA of SEP-856 has not been fully elucidated. However, the selective agonism of TAAR1 and 5-HT_{1A}, in addition to the lack of D_2/5-HT_{2A}–mediated efficacy, has the potential to translate into a significantly improved safety profile compared with available therapies, while still maintaining antipsychotic efficacy across a broad array of symptoms. Based on its unique MOA and preclinical profile in animals, SEP-363856 represents a promising candidate for the treatment of schizophrenia and potentially other neuropsychiatric disorders.

Acknowledgments

This manuscript is dedicated to the memory of a beloved colleague, Dr. Una C. Campbell.

Authorship Contributions

Participated in research design: Jones, Hopkins, Lew, Shao, J.E. Campbell, Spear, Large, U.C. Campbell, Hanania, Leahy, Koblan.

Conducted experiments: Jones, Lew, U.C. Campbell, J.E. Campbell, Hanania.

Performed data analyses: Dedic, Jones, Hopkins, Lew, J.E. Campbell, Large, U.C. Campbell, Hanania.

Wrote or contributed to the writing of the manuscript: Dedic, Jones, Hopkins, Lew, Large, Hanania, Koblan.

References

Alexandrov V, Brunner D, Hanania T, and Leahy E (2015) High-throughput analysis of behavior for drug discovery. *Eur J Pharmacol* **750**:82–89.

Belema M and Meanwell NA (2014) Discovery of daclatasvir, a pan-genotypic hepatitis C virus NS5A replication complex inhibitor with potent clinical effect. *J Med Chem* **57**:5057–5071.

Berke JD (2018) What does dopamine mean? *Nat Neurosci* **21**:787–793.

Black SW, Schwartz MD, Chen TM, Hoener MC, and Kilduff TS (2017) Trace amine-associated receptor 1 agonists as narcolepsy therapeutics. *Biol Psychiatry* **82**: 623–633.

Borowsky B, Adham N, Jones KA, Raddatz R, Artymyshyn R, Ogozalek KL, Durkin MM, Lakhlani PP, Bonini JA, Pathirana S, et al. (2001) Trace amines: identification of a family of mammalian G protein-coupled receptors. *Proc Natl Acad Sci USA* **98**:8966–8971.

Burchett SA and Hicks TP (2006) The mysterious trace amines: protean neuromodulators of synaptic transmission in mammalian brain. *Prog Neurobiol* **79**: 223–246.

Burnet PW, Eastwood SL, and Harrison PJ (1996) 5-HT1A and 5-HT2A receptor mRNAs and binding site densities are differentially altered in schizophrenia. *Neurop* **15**:442–455.

Burnet PWJ, Eastwood SL, and Harrison PJ (1997) [3H]WAY-100635 for 5-HT1A receptor autoradiography in human brain: a comparison with [3H]8-OH-DPAT and demonstration of increased binding in the frontal cortex in schizophrenia. *Neurochem Int* **30**:565–574.

Celada P, Bortolozzi A, and Artigas F (2013) Serotonin 5-HT1A receptors as targets for agents to treat psychiatric disorders: rationale and current status of research. *CNS Drugs* **27**:703–716.

Charpentier P, Gailliot P, and Jacob R (1952) Recherches sur les diméthylaminopropyl-N phénothiazines substituées. *Comptes rendus Acad Sci* **235**:59–60.

Christian SL and Berry MD (2018) Trace amine-associated receptors as novel therapeutic targets for immunomodulatory disorders. *Front Pharmacol* **9**:680.

de Almeida J and Mengod G (2008) Serotonin 1A receptors in human and monkey prefrontal cortex are mainly expressed in pyramidal neurons and in a GABAergic interneuron subpopulation: implications for schizophrenia and its treatment. *J Neurochem* **107**:488–496.

Espinoza S, Salahpour A, Masri B, Sotnikova TD, Messa M, Barak LS, Caron MG, and Gainetdinov RR (2011) Functional interaction between trace amine-associated receptor 1 and dopamine D2 receptor. *Mol Pharmacol* **80**:416–425.

Floresco SB, Yang CR, Phillips AG, and Blaha CD (1998) Basolateral amygdala stimulation evokes glutamate receptor-dependent dopamine efflux in the nucleus accumbens of the anaesthetized rat. *Eur J Neurosci* **10**:1241–1251.

Gainetdinov RR, Hoener MC, and Berry MD (2018) Trace amines and their receptors. *Pharmacol Rev* **70**:549–620.

Geyer MA, Krebs-Thomson K, Braff DL, and Swerdlow NR (2001) Pharmacological studies of prepulse inhibition models of sensorimotor gating deficits in schizophrenia: a decade in review. *Psychopharmacology (Berl)* **156**:117–154.

Girgis RR, Zoghbi AW, Javitt DC, and Lieberman JA (2019) The past and future of novel, non-dopamine-2 receptor therapeutics for schizophrenia: a critical and comprehensive review. *J Psychiatr Res* **108**:57–83.

Goonawardena AV, Morairty SR, Dell R, Orellana GA, Hoener MC, Wallace TL, and Kilduff TS (2019) Trace amine-associated receptor 1 agonism promotes wakefulness without impairment of cognition in Cynomolgus macaques. *Neuropsychopharmacology* **44**:1485–1493.

Harmeier A, Obermueller S, Meyer CA, Revel FG, Buchy D, Chaboz S, Dernick G, Wettstein JG, Iglesias A, Rolink A, et al. (2015) Trace amine-associated receptor 1 activation silences GSK3β signaling of TAAR1 and D2R heteromers. *Eur Neuropsychopharmacol* **25**:2049–2061.

Howes OD, Kambeitz J, Kim E, Stahl D, Slifstein M, Abi-Dargham A, and Kapur S (2012) The nature of dopamine dysfunction in schizophrenia and what this means for treatment. *Arch Gen Psychiatry* **69**:776–786.

Insel TR (2010) Rethinking schizophrenia. *Nature* **468**:187–193.

Ito H, Halldin C, and Farde L (1999) Localization of 5-HT1A receptors in the living human brain using [carbonyl-11C]WAY-100635: PET with anatomic standardization technique. *J Nucl Med* **40**:102–109.

Jauhar S, Veronese M, Rogdaki M, Bloomfield M, Natesan S, Turkheimer F, Kapur S, and Howes OD (2017) Regulation of dopaminergic function: an [^{18}F]-DOPA PET apomorphine challenge study in humans. *Transl Psychiatry* **7**:e1027.

Jones CA, Watson DJ, and Fone KC (2011) Animal models of schizophrenia. *Br J Pharmacol* **164**:1162–1194.

Jones JL, Day JJ, Aragona BJ, Wheeler RA, Wightman RM, and Carelli RM (2010) Basolateral amygdala modulates terminal dopamine release in the nucleus accumbens and conditioned responding. *Biol Psychiatry* **67**:737–744.

Karam CS, Ballon JS, Bivens NM, Freyberg Z, Girgis RR, Lizardi-Ortiz JE, Markx S, Lieberman JA, and Javitch JA (2010) Signaling pathways in schizophrenia: emerging targets and therapeutic strategies. *Trends Pharmacol Sci* **31**:381–390.

Kasper S, Tauscher J, Willeit M, Stamenkovic M, Neumeister A, Küfferle B, Barnas C, Stastny J, Praschak-Rieder N, Pezawas L, et al. (2002) Receptor and transporter imaging studies in schizophrenia, depression, bulimia and Tourette's disorder--implications for psychopharmacology. *World J Biol Psychiatry* **3**:133–146.

Kia HK, Miquel MC, Brisorgueil MJ, Daval G, Riad M, El Mestikawy S, Hamon M, and Vergé D (1996) Immunocytochemical localization of serotonin1A receptors in the rat central nervous system. *J Comp Neurol* **365**:289–305.

Kim E, Howes OD, Veronese M, Beck K, Seo S, Park JW, Lee JS, Lee YS, and Kwon JS (2017) Presynaptic dopamine capacity in patients with treatment-resistant schizophrenia taking clozapine: an [^{18}F]DOPA PET study. *Neuropsychopharmacology* **42**:941–950.

Kinon BJ, Millen BA, Zhang L, and McKinzie DL (2015) Exploratory analysis for a targeted patient population responsive to the metabotropic glutamate 2/3 receptor agonist pomaglumetad methionil in schizophrenia. *Biol Psychiatry* **78**:754–762.

Laborit H, Huguenard P, and Alluaume R (1952) Un nouveau stabilisateur végétatif; le 4560 RP. *Presse Med* **60**:206–208.
Lehmann HE and Ban TA (1997) The history of the psychopharmacology of schizophrenia. *Can J Psychiatry* **42**:152–162.
Leo D and Espinoza S (2016) *Trace Amine-Associated Receptor 1 Modulation of Dopamine System*, Elsevier.
Leo D, Mus L, Espinoza S, Hoener MC, Sotnikova TD, and Gainetdinov RR (2014) Taar1-mediated modulation of presynaptic dopaminergic neurotransmission: role of D2 dopamine autoreceptors. *Neuropharmacology* **81**:283–291.
Lieberman JA, Stroup TS, McEvoy JP, Swartz MS, Rosenheck RA, Perkins DO, Keefe RS, Davis SM, Davis CE, Lebowitz BD, et al.; Clinical Antipsychotic Trials of Intervention Effectiveness (CATIE) Investigators (2005) Effectiveness of antipsychotic drugs in patients with chronic schizophrenia. *N Engl J Med* **353**:1209–1223.
Lindemann L, Meyer CA, Jeanneau K, Bradaia A, Ozmen L, Bluethmann H, Bettler B, Wettstein JG, Borroni E, Moreau J-L, et al. (2008) Trace amine-associated receptor 1 modulates dopaminergic activity. *J Pharmacol Exp Ther* **324**:948–956.
Marsman A, van den Heuvel MP, Klomp DWJ, Kahn RS, Luijten PR, and Hulshoff Pol HE (2013) Glutamate in schizophrenia: a focused review and meta-analysis of ^{1}H-MRS studies. *Schizophr Bull* **39**:120–129.
Martin LP, Jackson DM, Wallsten C, and Waszczak BL (1999) Electrophysiological comparison of 5-hydroxytryptamine1A receptor antagonists on dorsal raphe cell firing. *J Pharmacol Exp Ther* **288**:820–826.
McCutcheon R, Beck K, Jauhar S, and Howes OD (2018) Defining the locus of dopaminergic dysfunction in schizophrenia: a meta-analysis and test of the mesolimbic hypothesis. *Schizophr Bull* **44**:1301–1311.
Meyer-Lindenberg A (2010) From maps to mechanisms through neuroimaging of schizophrenia. *Nature* **468**:194–202.
Miyamoto S, Duncan GE, Marx CE, and Lieberman JA (2005) Treatments for schizophrenia: a critical review of pharmacology and mechanisms of action of antipsychotic drugs. *Mol Psychiatry* **10**:79–104.
Miyamoto S, Leipzig JN, Lieberman JA, and Duncan GE (2000) Effects of ketamine, MK-801, and amphetamine on regional brain 2-deoxyglucose uptake in freely moving mice. *Neuropsychopharmacology* **22**:400–412.
Moffat JG, Vincent F, Lee JA, Eder J, and Prunotto M (2017) Opportunities and challenges in phenotypic drug discovery: an industry perspective. *Nat Rev Drug Discov* **16**:531–543.
Nestler EJ and Hyman SE (2010) Animal models of neuropsychiatric disorders. *Nat Neurosci* **13**:1161–1169.
Newman-Tancredi A (2010) The importance of 5-HT1A receptor agonism in antipsychotic drug action: rationale and perspectives. *Curr Opin Investig Drugs* **11**: 802–812.
Porsolt RD, Le Pichon M, and Jalfre M (1977) Depression: a new animal model sensitive to antidepressant treatments. *Nature* **266**:730–732.
Ratajczak P, Wozniak A, and Nowakowska E (2013) Animal models of schizophrenia: developmental preparation in rats. *Acta Neurobiol Exp (Warsz)* **73**:472–484.
Revel FG, Meyer CA, Bradaia A, Jeanneau K, Calcagno E, André CB, Haenggi M, Miss MT, Galley G, Norcross RD, et al. (2012a) Brain-specific overexpression of trace amine-associated receptor 1 alters monoaminergic neurotransmission and decreases sensitivity to amphetamine. *Neuropsychopharmacology* **37**:2580–2592.
Revel FG, Moreau J-L, Gainetdinov RR, Bradaia A, Sotnikova TD, Mory R, Durkin S, Zbinden KG, Norcross R, Meyer CA, et al. (2011) TAAR1 activation modulates monoaminergic neurotransmission, preventing hyperdopaminergic and hypoglutamatergic activity. *Proc Natl Acad Sci USA* **108**:8485–8490.
Revel FG, Moreau JL, Gainetdinov RR, Ferragud A, Velázquez-Sánchez C, Sotnikova TD, Morairty SR, Harmeier A, Groebke Zbinden K, Norcross RD, et al. (2012b) Trace amine-associated receptor 1 partial agonism reveals novel paradigm for neuropsychiatric therapeutics. *Biol Psychiatry* **72**:934–942.
Revel FG, Moreau JL, Pouzet B, Mory R, Bradaia A, Buchy D, Metzler V, Chaboz S, Groebke Zbinden K, Galley G, et al. (2013) A new perspective for schizophrenia: TAAR1 agonists reveal antipsychotic- and antidepressant-like activity, improve cognition and control body weight. *Mol Psychiatry* **18**:543–556.
Roberds SL, Filippov I, Alexandrov V, Hanania T, and Brunner D (2011) Rapid, computer vision-enabled murine screening system identifies neuropharmacological potential of two new mechanisms. *Front Neurosci* **5**:103.
Rutigliano G, Accorroni A, and Zucchi R (2018) The case for TAAR1 as a modulator of central nervous system function. *Front Pharmacol* **8**:987.
Samara MT, Dold M, Gianatsi M, Nikolakopoulou A, Helfer B, Salanti G, and Leucht S (2016) Efficacy, acceptability, and tolerability of antipsychotics in treatment-resistant schizophrenia: a network meta-analysis. *JAMA Psychiatry* **73**:199–210.
Schwartz MD, Black SW, Fisher SP, Palmerston JB, Morairty SR, Hoener MC, and Kilduff TS (2017) Trace amine-associated receptor 1 regulates wakefulness and EEG spectral composition. *Neuropsychopharmacology* **42**:1305–1314.
Schwartz MD, Canales JJ, Zucchi R, Espinoza S, Sukhanov I, and Gainetdinov RR (2018) Trace amine-associated receptor 1: a multimodal therapeutic target for neuropsychiatric diseases. *Expert Opin Ther Targets* **22**:513–526.
Shao L, Campbell UC, Fang QK, Powell NA, Campbell JE, Jones PG, Hanania T, Alexandrov V, Morganstern I, Sabath E, et al. (2016) In vivo phenotypic drug discovery: applying a behavioral assay to the discovery and optimization of novel antipsychotic agents. *MedChemComm* **7**:1093–1101.
Simpson MDC, Lubman DI, Slater P, and Deakin JFW (1996) Autoradiography with [3H]8-OH-DPAT reveals increases in 5-HT(1A) receptors in ventral prefrontal cortex in schizophrenia. *Biol Psychiatry* **39**:919–928.
Steeds H, Carhart-Harris RL, and Stone JM (2015) Drug models of schizophrenia. *Ther Adv Psychopharmacol* **5**:43–58.
Sumiyoshi T, Stockmeier CA, Overholser JC, Dilley GE, and Meltzer HY (1996) Serotonin1A receptors are increased in postmortem prefrontal cortex in schizophrenia. *Brain Res* **708**:209–214.
Swinney DC and Anthony J (2011) How were new medicines discovered? *Nat Rev Drug Discov* **10**:507–519.
Tauscher J, Kapur S, Verhoeff NP, Hussey DF, Daskalakis ZJ, Tauscher-Wisniewski S, Wilson AA, Houle S, Kasper S, and Zipursky RB (2002) Brain serotonin 5-HT(1A) receptor binding in schizophrenia measured by positron emission tomography and [11C]WAY-100635. *Arch Gen Psychiatry* **59**:514–520.
Tribl GG, Wetter TC, and Schredl M (2013) Dreaming under antidepressants: a systematic review on evidence in depressive patients and healthy volunteers. *Sleep Med Rev* **17**:133–142.
Wichniak A, Wierzbicka A, Walęcka M, and Jernajczyk W (2017) Effects of antidepressants on sleep. *Curr Psychiatry Rep* **19**:63.
Wilson CA, Koenig JI, and Psychiatric M (2015) Social interaction and social withdrawal in rodents as readouts for investigating the negative symptoms of schizophrenia. *Eur Neuropsychopharmacol* **24**:759–773.
Wolinsky TD, Swanson CJ, Smith KE, Zhong H, Borowsky B, Seeman P, Branchek T, and Gerald CP (2007) The trace amine 1 receptor knockout mouse: an animal model with relevance to schizophrenia. *Genes Brain Behav* **6**:628–639.
Yasuno F, Suhara T, Ichimiya T, Takano A, Ando T, and Okubo Y (2004) Decreased 5-HT1A receptor binding in amygdala of schizophrenia. *Biol Psychiatry* **55**:439–444.

Address correspondence to: Dr. Kenneth S. Koblan, Sunovion Pharmaceuticals, 84 Waterford Drive, Marlborough, MA 01752. E-mail: Kenneth.Koblan@Sunovion.com

Supplemental Information

SEP-363856, a novel psychotropic agent with a unique, non-D_2 receptor mechanism of action

Nina Dedic*, Philip G. Jones*, Seth C. Hopkins, Robert Lew, Liming Shao, John E. Campbell, Kerry L. Spear, Thomas H. Large, Una C. Campbell, Taleen Hanania, Emer Leahy, Kenneth S. Koblan

*both authors contributed equally to the work

The Journal of Pharmacology and Experimental Therapeutics

Supplemental Material and Methods

SmartCube® System for Behavioral Phenotypic Screening

The SmartCube® system is a mouse-based behavioral screening platform that combines proprietary hardware, computer vision algorithms and machine learning based data mining tools (Roberds *et al.*, 2011; Alexandrov *et al.*, 2015; Shao *et al.*, 2016). In order to create a reference database of therapeutic class signatures, various doses of clinically approved CNS drugs used to treat schizophrenia, depression, anxiety and other psychiatric disorders were screened. During a 45-minute automated test session, where mice are presented with multiple challenges, the behavioral responses of adult male C57Bl/6 mice (Taconic, Germantown, NY) treated with vehicle or test compounds were captured and analyzed using computer vision software and proprietary algorithms. During each test session over 2000 features are captured and the behavioral responses following treatment were compared to the database of reference drugs. SEP-856 was dissolved in vehicle (5% Pharmasolve; 30% PEG 200/ PEG 400/ propylene glycol; 65% saline) and administered i.p. (10 ml/kg) at dose levels of 0.1, 0.3, 1 and 10 mg/kg. Testing was initiated 15 minutes post-dosing.

PCP-Induced Hyperactivity

PCP-induced hyperactivity was assessed in open field chambers (27.3 x 27.3 x 20.3 cm; Med Associates Inc., St Albans, VT) surrounded by infrared photo beams (16 x 16 x 16) to measure horizontal and vertical activity. Distance travelled was measured from horizontal beam breaks. Adult, male C57Bl/6J mice (Jackson Laboratories, Bar Harbor, ME) were acclimatized to the experimental testing room for at least 1 hour prior to

testing. Mice were treated with vehicle (p.o.), SEP-856 (0.3, 1 and 3 mg/kg, p.o.) or clozapine (positive control; 1 mg/kg, i.p.) and placed in the open field chambers for 30 min measurement of baseline activity. Mice were then injected with either water or PCP (5 mg/kg, i.p.) and placed back in the open field chambers for a 60 min session. SEP-856 was dissolved in 20% hydroxypropyl-beta-cyclodextrin and clozapine in 10% DMSO. PCP was dissolved in sterile injectable water. The dosing volume for all treatments was 10 ml/kg. The open field chambers were cleaned following each test. Data were analyzed using one-way ANOVA followed by Tukey's post-hoc test ($p < 0.05$).

Prepulse Inhibition (PPI)

The acoustic startle measures an unconditioned reflex response to external auditory stimulation. PPI, consisting of an inhibited startle response (reduction in amplitude) to an auditory stimulation following the presentation of a weak auditory stimulus or prepulse, has been used to assess deficiencies in sensory-motor gating, such as those seen in schizophrenia. Mice were placed in the PPI chambers (Med Associates) for a 5-minute session of white noise (70 dB) habituation after which the test session was automatically started. The session started with a habituation block of 6 presentations of the startle stimulus alone, followed by 10 PPI blocks of 6 different types of trials. Trial types are: null (no stimuli), startle (120 dB), startle plus prepulse (4, 8 and 12 dB over background noise i.e. 74, 78 or 82 dB) and prepulse alone (82 dB). Trial types were presented at random within each block. Each trial started with a 50 ms null period during which baseline movements are recorded. There was a subsequent 20 ms period

during which prepulse stimuli were presented and responses to the prepulse measured. After further 100 milliseconds the startle stimuli were presented for 40 milliseconds and responses recorded for 100 milliseconds from startle onset. Responses were sampled every ms. The inter-trial interval was variable with an average of 15 seconds (range from 10 to 20 seconds). In startle alone trials the basic auditory startle was measured, and in prepulse plus startle trials the amount of inhibition of the normal startle was determined and expressed as a percentage of the basic startle response (from startle alone trials), excluding the startle response of the first habituation block.

Adult, male C57Bl/6J mice (Jackson Laboratories, Bar Harbor, ME) were acclimatized to the experimental room for at least 1 hour prior to testing. SEP-856 (0.3, 1, 3, 10 and 30 mg/kg, p.o.) was formulated in 20% hydroxypropyl-beta-cyclodextrin (vehicle) and haloperidol (1 mg/kg, i.p.) in 10% DMSO. The dosing volume for all treatments was 10 ml/kg and animals were dosed 30 min prior to testing. The PPI enclosures were cleaned following each test. Data were analyzed using one-way ANOVA followed by Tukey's post-hoc test ($p < 0.05$).

PCP-Induced Deficits in Social Interaction

For five days prior to test, male Sprague-Dawley rats (~ 150 g on arrival from Harlan Laboratories, IN) were injected twice daily with either PCP (2 mg/kg; s.c.) or saline (s.c.). On day 6, after acute pretreatment (30 min) with either water (p.o.), clozapine (2.5 mg/kg, i.p.) or SEP-856 (1, 3 and 3 mg/kg, p.o.) a pair of unfamiliar rats, receiving the same treatment were placed in a white plexiglass open field arena (24" x 17" x 8") and allowed to interact with each other for 6 minutes. Social interactions ('SI') included:

sniffing the other rat; grooming the other rat; climbing over or under or around the other rat; following the other rat; or exploring the ano-genital area of the other rat. Passive contact and aggressive contact were not considered a measure of social interaction. The time the rats spent interacting with each other during the 6-minute test was recorded by a trained observer blinded to drug treatment and condition. The social interaction chambers were thoroughly cleaned after each test session. Twenty animals were tested in each group for a final number of ten interactions. PCP, clozapine and SEP-856 were dissolved in saline, 5%PEG/5%Tween80 in saline, and sterile injectable water respectively. All treatments were administered at a dosing volume of 1ml/kg. Data were analyzed using one-way ANOVA followed by Tukey's post-hoc test ($p < 0.05$).

Forced Swim Test

The forced swim test consisted of one 6-minute session of forced swimming in individual opaque cylinders (15 cm tall x 10 cm wide, 1000 ml beakers) containing fresh tap water at a temperature of 23 $\pm$ 2 °C and a depth of 12 cm (approximately 800 ml) for each test animal. The time the animal spent immobile was recorded over the 6-minute trial. Every one minute, the cumulative immobility time was recorded from the start of the session and noted on the study data record sheet. Immobility was defined as the postural position of floating in the water. The animals are generally observed with the back slightly hunched and the head above water with no movements or with small stabilizing movements of the limbs. Sometimes the back is arched with the animal stretched across the sides of the beaker, and in this posture, immobility was recorded only if the animal was not struggling. Adult, male BalbC/J mice (Jackson Laboratories,

Bar Harbor, ME) were tested 60 minutes post administration of vehicle (sterile injectable water; p.o.), or SEP-856 (0.3, 1, 3 and 10 mg/kg, p.o.) and 30 minutes post sertraline (positive control; 20 mg/kg, i.p.) injection. All treatments were formulated in sterile injectable water and administered at a dosing volume of 10 ml/kg. Data are represented as the time the mice spent immobile during the 6-minute trial. Data were analyzed using one-way ANOVA followed by Tukey's post-hoc test ($p < 0.05$).

Catalepsy

Catalepsy was assessed using the bar test in adult, male C57Bl/6J mice (Jackson Laboratories, Bar Harbor, ME). The front paws of a mouse were placed on a horizontal metal bar raised 2" above a Plexiglas platform and time was recorded for up to 30 seconds per trial. The test ended when the animal's front paws returned to the platform or after 30 seconds. The test was repeated three times and the average of the trials is reported as the intensity index of catalepsy. Mice were acclimatized to the experimental room for at least one hour prior to testing. Catalepsy was assessed at 30 minutes and 90 minutes following vehicle (20% hydroxypropyl-beta-cyclodextrin, p.o.), haloperidol (1 mg/kg, i.p.) or SEP-856 (100 mg/kg, p.o.) administration. Haloperidol and SEP-856 were dissolved in 20% hydroxypropyl-beta-cyclodextrin and 10% DMSO respectively and administered at a volume of 10 ml/kg. At the end of each trial, the apparatus was thoroughly cleaned with 70% ethanol. Data were analyzed using two-way ANOVA followed by Tukey's post-hoc test ($p < 0.05$).

Electroencephalograph (EEG) Recordings

Seven male Sprague-Dawley rats (300 ± 25 g; Charles River, Wilmington, MA) were implanted with chronic recording devices for continuous recordings of EEG, electromyograph (EMG), core body temperature (Tb), and locomotor activity (LMA) via telemetry. Under isoflurane anesthesia (1–4%), a dorsal midline incision on top of the head and a midventral incision along the linea alba through the peritoneum were made. Sterile miniature transmitters (F40-EET, Data Sciences Inc., St Paul, MN) were inserted through the peritoneal incision and sewn to the musculature with a single stitch of silk suture (4-0). Four biopotential leads from the transmitters were inserted subcutaneous into the neck and head region. Two holes were drilled through the skull, one at –5.0 mm AP and 4.0 mm ML and the other at 2.0 mm AP and 2.0 mm ML from bregma. The two biopotential leads used as EEG electrodes were inserted into the holes and affixed to the skull with dental acrylic. The two biopotential leads used as EMG electrodes were sutured into the neck musculature. The incision was closed with suture (silk 4-0) and antibiotics were administered topically. Pain was relieved by a long-lasting analgesic (buprenorphine) administered intramuscularly postoperatively. After surgery, animals were placed in a clean cage and observed until they recovered. EEG, EMG, Tb, and LMA were recorded via telemetry using DQ ART 4.1 software (Data Sciences Inc., St Paul, MN). Animals were acclimated to the handling procedures and were given two separate 1 ml administrations of vehicle by oral gavage, one 7 days and the other 3 days before the first experimental day. Following completion of the data collection, expert scorers determined states of sleep and wakefulness in 10 second (s) epochs by examining the recordings visually using NeuroScore software (Data Sciences Inc., St

Paul, MN). All doses of SEP-856 (1, 3 and 10 mg/kg), caffeine (10 mg/kg), and vehicle were administered by oral gavage with a minimum of 3 days between successive treatments. Doses were administered at the start of Zeitgeber hour 7 (ZT7; i.e. 6 hours after light on) and the following 6 hours of continuous EEG and EMG recordings were analyzed. EEG and EMG data were scored visually in 10 second epochs for wakes (W), REM, and non-REM (NREM). Scored data were analyzed and expressed as time spent in each state per hour. Latency to NREM onset for each rat was calculated from the time of drug administration to the first six continuous 10 second epochs scored as NREM. Latency to REM onset for each rat was calculated from the time of drug administration to the first three continuous 10 second epochs scored as REM. Cumulative time spent in W, NREM, and REM, as well as the REM:NREM ratios, were calculated for the 6-hour recording period. Tb and LMA (counts per minute) were analyzed as mean values per hour (hourly means).

In Vivo Microdialysis

Male Sprague-Dawley rats (240-325 g; Harlan, Frederick, MD) were allowed to acclimate to the facility for at least 5 days before surgery.

Microdialysis experiment: Two days prior to test article administration, rats were anesthetized with a mixture of ketamine/xylazine (70 mg/kg/6 mg/kg, i.m) and placed in a stereotaxic instrument. Microdialysis probes (CMA/12; 4 mm membranes) were then implanted in the striatum and/or prefrontal cortex. The coordinates from bregma for striatum were +0.9 mm anterior-posterior, +3 mm medio-lateral; -7.5 mm dorso-ventral and for prefrontal cortex, +3.4 mm anterior-posterior, -0.6 mm medio-lateral; -5.5 mm

dorso-ventral. Probes were secured to the skull with cranioplastic cement (Henry Schein) and three screws. Once conscious, rats received a single dose of ketoprofen (10 mg/kg, s.c) for analgesia. 24 to 28 hours after the surgery, rats were placed under light isoflurane anesthesia in order to connect the microdialysis probes to the perfusion pumps using sterile polyethylene tubing. Rats were then placed in microdialysis chambers (with free access to food and water) and artificial cerebrospinal fluid (aCSF; CMA) was perfused through the probes at a flow rate of 0.5 µL/min overnight. Approximately 14-16 hours later, on the day of test article administration, the probe perfusion flow rate was increased to 1.5 µL/min and a 2-hour equilibration period was allowed before sample collection began. Microdialysate samples were collected every 30 minutes using tubes containing 10 µL of formic acid (0.5M) in refrigerated fraction collectors, to prevent monoamine degradation. Four baseline samples were collected at 30-minute intervals over a 2-hour period before rats were dosed orally (2 mL/kg, via gavage) with SEP-856 or vehicle. SEP-856 was administered at 3, 10 and 30 mg/kg p.o. in saline. Eight samples were collected at 30-minute intervals over a 4-hour period after test article administration. Animals were awake and freely moving throughout the experiment. Rats were returned to their home cage at the end of the microdialysis experiment and sacrificed by decapitation within 72 hours. Brains were immediately removed and frozen using isopentane in dry ice and stored at -80ºC until histological verification of probe placement.

Sample analysis: Monoamine levels in perfusate samples from either brain area were analyzed by HPLC-EC detection within 24 hours of the microdialysis experiment. On

every experimental day, HPLC instruments were calibrated using freshly prepared standards containing known concentrations of dopamine (DA) and serotonin (5HT) (0; 0.05; 0.1; 1; 2 and 5 pg/µL of aCSF). For each concentration, 45 µL of standards in aCSF were added to 10 µL of formic acid (0.5M) in order to reproduce the dialysate sample conditions. DA and 5HT levels in the striatum were measured by transferring the dialysate samples to an autosampler (ESA, Inc. Model 540). 27 µL were injected onto a Capcell Pak column (250 × 1.5 mm, 3 µm particle size; ESA MD-160). DA and 5HT were eluted using a mobile phase consisting of 150 mM ammonium acetate and 140 µM EDTA in 15% methanol and 5% acetonitrile, pH 6.0. DA and 5HT were detected with a glassy carbon target analytical cell (ESA 5041) at a potential of 220mV using a Coulochem III detector (ESA). Chromatography data was acquired on a PC and analyzed using the EZ Chrome Elite software (Agilent technologies). DA and 5HT were measured in dialysate samples from the prefrontal cortex using the Alexys 100 system (Antec Leyden). Samples were transferred onto an autosampler (AS 100Antec Leyden) and a 30 µL injection was split equally between 2 columns. DA and 5HT were eluted with a C18 column (50 × 1 mm, 3 µm particle size; Antec Leyden ALB-105). The mobile phase for either column consisting in 50 mM phosphoric acid, 8 mM KCl, 0.1 mM EDTA and 500 mg/L OSA in 4 to 7% MeOH, pH 6.0. DA and 5HT were detected with a 0.7 mm glassy carbon electrode cell (VT-03, Antec Leyden) at a potential of 300 mV. Chromatography data were acquired on a PC and analyzed using the Alexys software (Antec Leyden).

In Vivo Pharmacokinetic Studies

Pharmacokinetic studies were conducted in male ICR mice (21.2 to 24.4 g; Shanghai Laboratory Animal Center), male Sprague-Dawley rats (212 to 235 g; Shanghai Laboratory Animal Center) and male rhesus monkeys (~ 3.75 years of age). In all studies SEP-856 was formulated in phosphate buffered saline (pH 7 – 7.4) for oral or i.v. administration to animals that were fasted overnight. To determine brain penetration, mice or rats were dosed orally with 10 mg/kg SEP-856 and blood and brain collected at various timepoints from 15 min to 24 hours (n = 3/timepoint) after drug administration. Blood samples were collected by cardiac puncture following euthanasia by CO_2 inhalation, placed into K_2EDTA tubes and centrifuged at 8,000 rpm for 6 minutes at 4^0C, and the plasma extracted and frozen at -80^{o}C. Brains were removed, placed on ice and rinsed with saline prior to freezing at -80^{o}C. The PK properties of SEP-856 were determined in rats dosed with 10 mg/kg (i.v.) or 50 mg/kg (p.o.) SEP-856 and in rhesus monkeys dosed with 5 mg/kg SEP-856 (i.v. or p.o.). Serial blood samples were collected at various timepoints ranging from 5 min to 24 hours post dose (n = 3 subjects). Concentrations of SEP-856 were determined by high performance liquid chromatography with mass spectrometric detection. The lower limits of quantification were 2.5 ng/ml for plasma and 5 ng/g for brain and pharmacokinetic parameters were calculated using WinNonlin Pro version 5.0 or 5.2 (Pharsight Corporation, USA). Any concentrations that were below the limit of quantification were omitted from the calculation of pharmacokinetic parameters in individual animals.

In Vitro Autoradiography

In vitro autoradiography was used to determine the effects of SEP-856 on [^{3}H]-8-OH-DPAT binding to 5-HT$_{1A}$ receptors in brain sections of adult Sprague-Dawley rats (Harlan, Frederick, MD). Briefly, slide mounted rat brain sections (12 µm) consisting of prefrontal cortex (PFC), cortex (motor and somatosensory), septum, striatum, dorsal hippocampus and hypothalamus were preincubated for 30 minutes in 50 mM tris buffer (pH 7.5) at room temperature. Sections were then incubated in the same buffer containing 4 mM $CaCl_2$; 0.1% ascorbic acid pH 7.5 containing 2 nM [^{3}H]-8-OH-DPAT in the absence (total binding) and presence of SEP-856 (100 nM, 1 uM or 10 µM) for one hour at room temperature (22 -25 ˚C). Non-specific binding was defined by 10 µM 5-HT. Following incubation, slices were briefly rinsed, then washed in ice cold incubation buffer for 2 x 10 minutes. Brain sections were then rinsed in ice cold H_2O and dried under a stream of cool air. Rat brain sections were imaged by placing the tissue sections in a Biospace β-Imager for 6 hours. Afterwards, [^{3}H]-8-OH-DPAT binding in the absence and presence of SEP-856 was quantified using software provided by Biospace and the effect of SEP-856 on [^{3}H]-8-OH-DPAT binding to 5-HT$_{1A}$ receptors was determined. In a follow up experiment, the above experimental design was repeated using rat brain sections containing cortex and septum. Following image quantification, Graphpad Prism software was used to determine the IC_{50} of SEP-856.

D_2 Receptor Occupancy in Rats

The occupancy of D_2 receptors after i.p. administration of SEP-856 was evaluated in male Sprague-Dawley rats (216-232 g; Harlan, Frederick, MD). SEP-856 (10 mg/kg, 2

ml/kg) or vehicle (20% HPβCD) were administered i.p. at t = 0. [^{3}H]-raclopride (60 µCi/kg) was administered i.v. at t = 30 min and rats were killed by rapid decapitation at t = 60 min. Brains were frozen in isopentane (previously cooled on dry ice) and stored at -80ºC until required for cryosectioning. Blood samples were processed to obtain plasma samples which were then stored at -80ºC until required for exposure analysis. For cryosectioning, brains were removed from the -80ºC freezer and allowed to thaw to -20ºC. Coronal sections (20 µm) of the striatum (region of interest) and cerebellum (reference region) were cut and thaw mounted onto glass microscope slides. Slide mounted tissue sections (of striatum and cerebellum) were placed in the Biospace β-Imager and imaged for 6 hours. Images were quantitated using software (Betavision plus) provided by Biospace and a signal:noise (striatum:cerebellum) value was determined for each animal. The percent receptor occupancy was determined using the following equation:

$$\%RO = 100 \times [(\text{average } S{:}N_{Vehicle}) - S{:}N_{Subject}] / [(\text{average } S{:}N_{Vehicle}) - 1]$$

A satellite group of rats was also used for determination of SEP-856 exposures in the plasma and brain. Rats received SEP-856 (10 mg/kg, 2 ml/kg, i.p.). 60 minutes later, rats were euthanized by CO_2 inhalation. Rats were then decapitated, and brains and plasma samples collected. Brain and plasma samples were analyzed for drug concentration using LC/MS analysis.

<u>D_2 Receptor Occupancy in Nonhuman Primates</u>

Positron Emission Tomography (PET) imaging was conducted in two nonhuman primate female baboons (*Papio anubis*; ~18 kg) to study the effect of SEP-856 on D_2

receptors: one dose (~7.25 mg/kg) was tested in duplicate. Prior to injection, quality control of the radiopharmaceutical was performed to ensure purity, identity, strength and sterility. A blockade protocol design was used to estimate the receptor occupancy where SEP-856 was administered 30 minutes prior to [^{18}F]-fallypride injection. A baseline study (no blocking agent) was also conducted with [^{18}F]-fallypride for each animal. The animals were fasted for 18–24 hours before the study and were anesthetized with intramuscular ketamine at 10 mg/kg and glycopyrrolate at 0.01 mg/kg (at 2 hours prior to radiopharmaceutical injection for the imaging studies), transferred to the PET camera for the imaging studies, and intubated with an endotracheal tube for continued anesthesia with 2.5% isoflurane administered through a rebreathing circuit. Body temperature was kept at 37 °C using a heated water blanket. Vital signs, including heart rate, blood pressure, respiration rate, oxygen saturation and body temperature, were monitored every 10 to 20 min during the study. An intravenous line was placed and used for injection of the radiopharmaceutical [^{18}F]-fallypride and the test article SEP-856 for the blockade studies. For the latter, the animal was injected with SEP-856 as a bolus over 5 min at T = 0 min and with the radiotracer [^{18}F]-fallypride at T = 30 minutes. Following the intravenous injection of [^{18}F]-fallypride as a bolus over 3 min at T = 30 minutes, a series of 45 dynamic 3D PET scans were obtained continuously on a Biograph mCT camera over three hours (T = 30 – 210 minutes) as follows: 6 x 30 seconds, 3 x 1minutes, 2 x 2 minutes, 34 x 5 minutes. The dynamic series were subsequently reconstructed using iterative reconstruction with corrections for random, scatter, and attenuation provided by the camera manufacturer. Reconstructed PET image data volumes were transferred to the image processing PMOD software package

(PMOD Technologies, Zurich, Switzerland) where the images were realigned onto the monkey MR to apply a volume of interest (VOI) template comprising the following regions: caudate, putamen, globus pallidus and cerebellum. Average activity concentration (kBq/cc) within each VOI was determined and time activity curves (TAC) were generated for each study, depicting the regional brain activity concentration over time (total uptake = specific plus non-displaceable). Time activity curves were expressed in SUV units (g/mL) by normalizing by the animal weight and the injected dose. The non-invasive reference region models SRTM, SRTM2 and Logan noninvasive using the cerebellum as reference region were applied to the regional time activity curves with the PMOD software to determine the binding potential BPND for each region mentioned above. For SRTM2, k'2 was estimated by doing a coupled fit across the caudate, putamen and globus pallidus. For Logan, the k'2 obtained from the SRTM2 coupled fit was used. The occupancy was determined using the binding potential BPND as follows: Occ = ((BP_{ND}Baseline – BP_{ND}Drug)/BP_{ND}Baseline). Similar results were obtained with all three non-invasive reference region models (SRTM, SRTM2 and Logan noninvasive). Thus, only the values obtained with the SRTM model are shown in the results.

Whole-Cell Patch Clamp Recordings in the DRN and VTA

Male C57BL/6 mice (4-16 weeks,15-35 g) were humanely killed by terminal anesthesia with isoflurane, cervical dislocation, and decapitation. The brain was then removed and 300 µm thick sagittal slices containing the VTA and/or the DRN were sectioned using a Leica VT1000S. After brain removal and throughout slicing the tissue was submerged in

ice cold (< 4°C) 'high sucrose' artificial cerebrospinal fluid (aCSF) of the following composition (in mM): Sucrose, 154; KCl, 1.9; KH_2PO_4, 1.2; $CaCl_2$, 0.1; $MgCl_2$, 3.6; $NaHCO_3$, 26; D-glucose, 10; L-ascorbic acid, 0.3; equilibrated with 95% O_2-5% CO_2. Once slices were cut, they were transferred to a beaker containing 'standard' aCSF and left at room temperature for a minimum of one hour before commencing electrophysiological recordings. After this period, individual slices were transferred to a custom-built recording chamber continuously perfused with 'standard' aCSF at a rate of 4–10 ml/min. 'Standard' aCSF composition (in mM): NaCl, 127; KCl, 1.9; KH_2PO_4, 1.2; $CaCl_2$, 2.4; $MgCl_2$, 1.3; $NaHCO_3$, 26; D-glucose, 10; equilibrated with 95% O_2-5% CO_2. Whole-cell patch-clamp recordings were performed at room temperature using the 'blind' version of the patch-clamp technique with either Axopatch 1D or Multiclamp 700B amplifiers. Patch pipettes were pulled from thin-walled borosilicate glass with resistances of between 3 and 8 MΩ when filled with intracellular solution of the following composition (mM): potassium gluconate, 140; KCl, 10; EGTA-Na, 1; HEPES, 10; Na2-ATP, 2, 0.3 GTP with pH and osmolarity compensated with KOH and sucrose, respectively. Recordings were monitored on an oscilloscope and a PC running Axon pClamp software and digitized at 2-10 kHz. At the beginning of each whole-cell patch-clamp recording, a current/voltage (IV) relationship was performed to identify active conductances in the recorded neuron, before testing the effects of SEP-856 and TAAR1/5-HT_{1A} receptor ligands. Changes in electrophysiological parameters including membrane potential and neuronal firing rate were analyzed using Axon pClamp and Microsoft Excel software to measure the effects of test compounds. To attempt neuronal phenotype characterization, DRN neurons were classified as being either sensitive or

insensitive to administration of the 5-HT_{1A} receptor agonist 8-OH-DPAT. In addition, after the determination of repeatable responses, administration of SEP-856 was repeated in the presence of the selective TAAR1 antagonist EPPTB and/or the selective 5-HT_{1A} receptor antagonist WAY-100635. Compound concentrations were chosen based on the results of pilot concentration-response whole-cell patch clamp recordings in the VTA and DRN. Changes in neuronal properties are presented as mean ± S.E.M and, in some cases, calculated as a percentage of control by calculating the mean of the normalized response. Where appropriate, statistical comparisons have been performed using the paired student's t-test, with $P < 0.05$ taken to indicate statistical significance.

In Vivo Extracellular Single-Unit Recordings in the DRN

Male Sprague-Dawley rats (275-400 g; Harlan, IN) were anesthetized with Urethane (initial dose at 1.2 to 1.6 g/kg, i.p.) and were surgically implanted with two catheters, one for femoral vein (drug administration) and one for femoral artery (blood sampling). The animals were then mounted on a stereotaxic apparatus (David Kopf instrument) in a flat skull position. Proper surgical anesthesia was maintained throughout the experiment by administration of supplemental doses of the anesthetic. Core temperature was maintained at 37ºC by a heating pad. Borosilicate glass micropipette electrodes (3 mm OD, 2 mm ID, Sutter Instrument) were pulled by PE-22 micro-electrode puller (Narishige Group) and then filled with 0.5% sodium acetate in 2% Pontamine Skyblue (Sigma). The electrodes had in vitro impedances of 1-3 MΩ. To gain access to dorsal raphe nucleus recording site the micro-electrode was advanced by a single axis in vivo

micromanipulator (Scientifica, United Kingdom) mounted on Kopf stereotaxic holders. One burr hole was drilled on the skull with stereotaxic coordinate of AP-7.8 mm, lateral 0.8 mm. The dura was carefully removed to expose the cortical surface. The recording electrode was inserted into brain through the hole at a 10-degree angle towards midline and advanced to reach the target coordinate of raphe nucleus (5.1-6.1 mm below the brain surface).

Extracellular single-unit activities were amplified (x1000), filtered (low pass 3 KHz and high pass at 300 Hz), displayed on the oscilloscope and stored in a computer equipped with the Spike 2 analysis system (Cambridge Electronic Design, UK) for off-line analysis. The recorded neurons location was histologically confirmed. Based on previous reports, the neurons which met the following criteria were included for the study: Slow firing rate (0.1 to 5 Hz), exhibiting a long duration (2-4 ms), single or bursting patterned action potentials with biphasic or triphasic extracellular waveforms (Aghajanian *et al.*, 1978; Clifford *et al.*, 1998; Hajós *et al.*, 2007). The baseline firing activity of the neuron was recorded for at least 10 min prior to the compound administration. SEP-856 was tested at 1, 2, and 5 mg/kg by i.v. injection. After clear inhibitory effects were observed (3-5 minutes after compound administration), WAY-100635 (0.08 mg/kg, i.v.) was given to determine whether it could antagonize the inhibitory effect of SEP-856. This dose range was previously reported to reverse the inhibitory effects of 8-OH-DPAT (Martin *et al.*, 1999). All test substances were dissolved in sterile saline and administered i.v. at a dose volume of 1 ml/kg. Blood samples were taken 30 min following compound administration. At the end of each experiment, the recording site was marked by the microiontophoresis of pontamine skyblue (-20 μA, 15

min). Each rat was then given an overdose of urethane. The brains were immediately removed, were frozen on dry ice, and were cut into 40 µM thick coronal sections using a cryostat. The sections were mounted on gelatin-coated slides and stained with cresyl violet in order to determine the location of the recording sites.

In Vitro Binding Studies

Equilibrium radioligand binding was performed using the following incubation conditions:

5-HT_{1A}: Membranes from HEK-293 cells expressing the human recombinant 5-HT_{1A} receptor were incubated in the presence of 0.3 nM [^{3}H]-8-OH-DPAT for 60 minutes at 22˚C.

5-HT_{1B}: Rat cerebral cortex membranes were incubated with 0.1 nM [^{125}I]-CYP for 120 minutes at 37°C.

5-HT_{1D}: Membranes from CHO cells expressing the rat recombinant 5-HT_{1D} receptor were incubated in the presence of 1 nM [^{3}H]-5-HT for 60 minutes at 22°C.

5-HT_{2A}: Membranes from HEK-293 cells expressing the human recombinant 5-HT_{2A} receptor were incubated in the presence of 0.1 nM [^{125}I]-(±)DOI for 60 minutes at 22°C.

5-HT_{2B}: Membranes from HEK-293 cells expressing the human recombinant 5-HT_{2B} receptor were incubated in the presence of 0.2 nM [^{125}I]-(±)DOI for 60 minutes at 22°C.

5-HT_{2C}: Membranes from HEK-293 cells expressing the human recombinant 5-HT_{2C} receptor were incubated in the presence of 0.1 nM [^{125}I]-(±)DOI for 60 minutes at 37°C.

5-HT_{7}: Membranes from HEK-293 cells expressing the human recombinant 5-HT_{7} receptor were incubated in the presence of 4 nM [^{3}H] LSD for 120 minutes at 22°C.

D_2: Membranes from HEK-293 cells expressing the human recombinant D_2 receptor were incubated in the presence of 0.3 nM [^{3}H]-methylspiperone for 60 minutes at room temperature.

α_{2A}: Membranes from HEK-293 cells expressing the human recombinant α_{2A} receptor were incubated in the presence of 0.3 nM [^{3}H]-methylspiperone for 60 minutes at room temperature.

Supplemental Figures

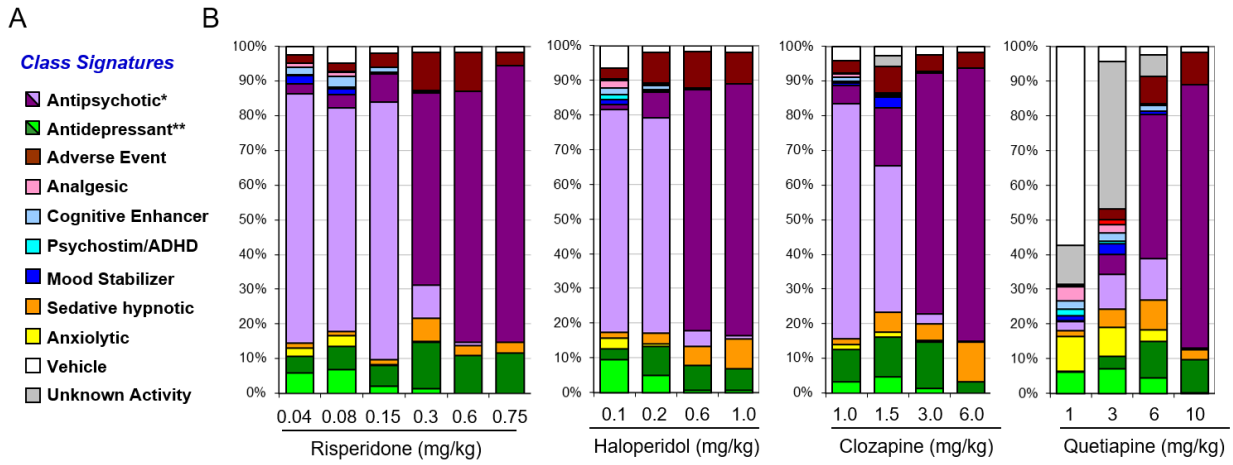

Supplemental Figure 1. SmartCube® behavioral signatures of typical and atypical antipsychotic drugs in mice. (A) Behavioral class signature color key representing 15 classes (*antipsychotic (purple) and high-dose antipsychotic (dark purple); **antidepressant (green) and *high-dose antidepressant (dark green)). (B) The predominant purple color is characteristic of an antipsychotic signature as shown for different doses of risperidone, haloperidol, clozapine and quetiapine (administered i.p. 15 min before testing, n = 6-8/dose).

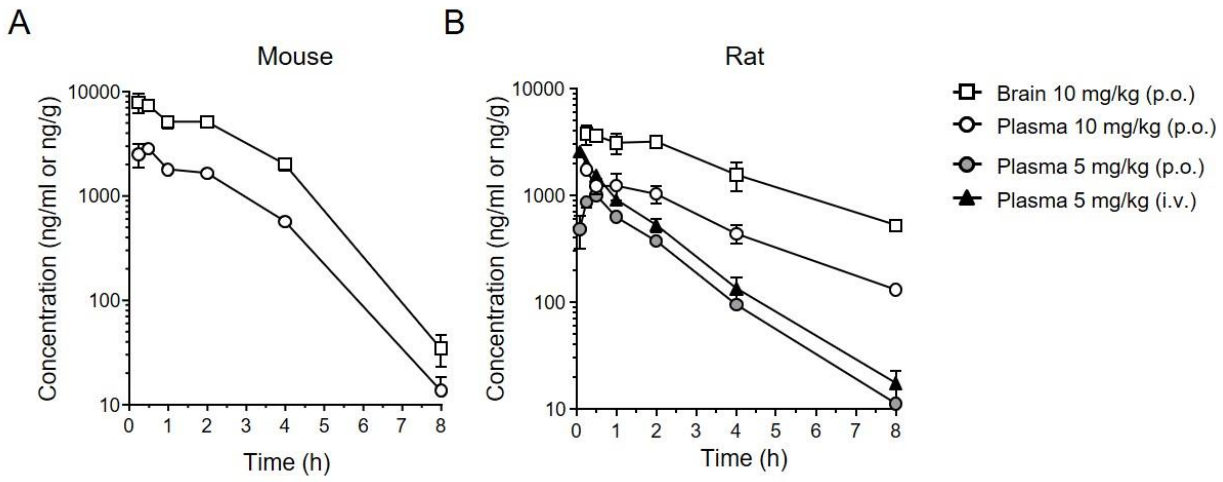

Supplemental Figure 2**.** SEP-856 exhibits good brain penetrance and rapid absorption in rodents**.** SEP-856 was administered orally and/or intravenously to male (A) ICR mice and (B) Sprague-Dawley rats. Plasma and brain samples were taken from n = 3 animals at each of the time points indicated. The brain-to-plasma AUC ratios for the 10 mg/kg dose ranged from 2.58 to 3.54 and 2.1 to 3.9 in mice and rats, respectively. Data are shown as mean ± s.e.m.

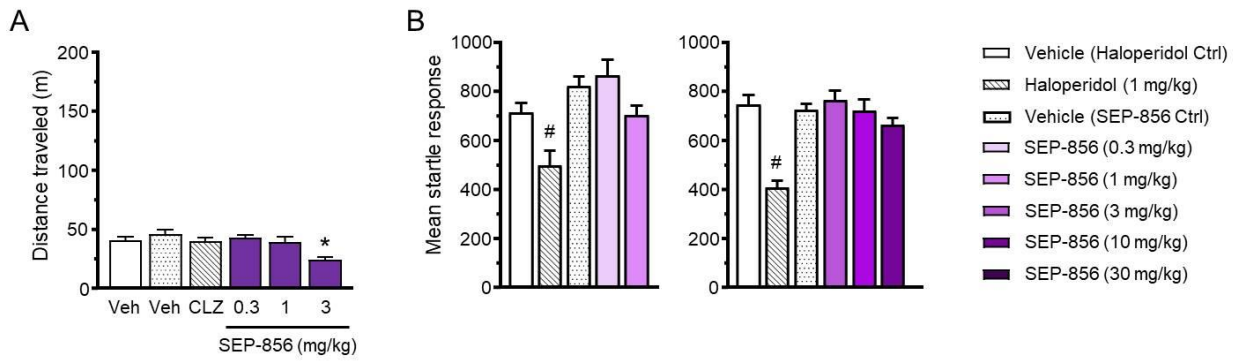

Supplemental Figure 3. Effect of SEP-856 on baseline locomotion and the acoustic startle response in C57Bl/6J mice. (A) At the highest tested dose (3 mg/kg), oral SEP-856 administration led to a slight reduction in overall activity during the open field test (one-way ANOVA $F_{(5, 59)} = 5.5$, $p = 0.0003$; Tukey's post-hoc test, * $p < 0.05$ vs. Veh (second bar from the left)). Clozapine (CLZ) tested at 1 mg/kg i.p. had no significant effect on locomotion. First vehicle (20% cyclodextrin, i.p.); second vehicle (20% cyclodextrin, p.o.). (B) The acoustic startle response, measured during the PPI test, was not significantly affected by SEP-856 (p.o.) compared to the respective vehicle control. In contrast, Haloperidol (i.p.) produced a significant reduction in the mean startle response (one-way ANOVA for the first experiment: $F_{(4, 42)} = 8.5$, $p < 0.0001$; second experiment: $F_{(5, 49)} = 11.5$, $p < 0.0001$; Tukey's post-hoc test, * $p < 0.05$ vs. Veh; n = 8-10/group). Vehicle for haloperidol (10% DMSO, i.p.), vehicle for SEP-856 (20% cyclodextrin, p.o.). Data are shown as mean ± s.e.m.

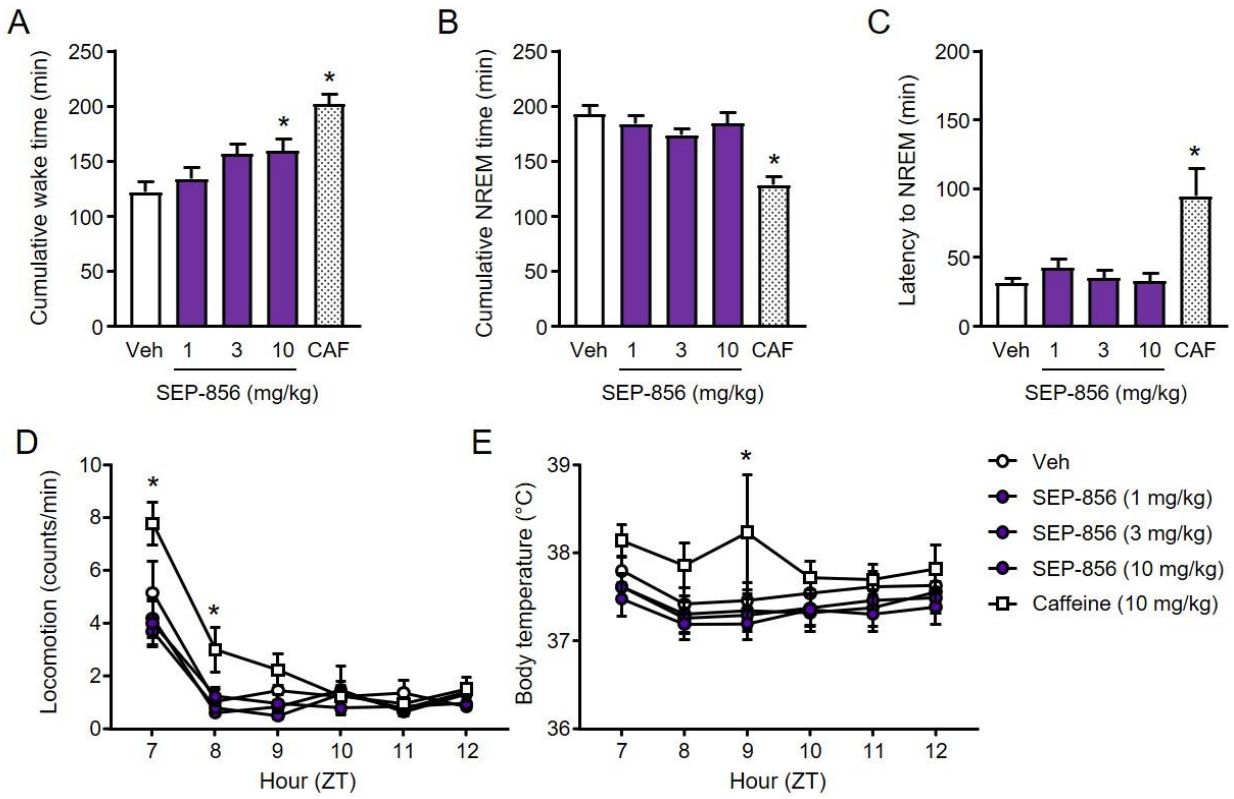

Supplemental Figure 4. Effects of SEP-856 on sleep/wake architecture in Sprague-Dawley rats. (A) Acute, oral administration of SEP-856 led to a significant increase in cumulative wake time at 10 mg/kg over the 6-hour recording period (one-way repeated-measures ANOVA + two-tailed t-test, *p < 0.05 vs. Veh). Cumulative NREM (B), latency to NREM (C), locomotor activity (D) and body temperature (E) were not significantly affected by SEP-856 during the 6-hour recording period (two-way repeated-measures ANOVA + two-tailed t-test, *p < 0.05 vs. Veh). The positive control caffeine (CAF, 10 mg/kg, p.o.) produced an expected increase in cumulative wake time, decrease in cumulative NREM time, increase in the latency to NREM as well as an increase in locomotion and body temperature. Dosing occurred in the middle of the resting phase, at the beginning of Zeitgeber time 7. N = 7. Data are shown as mean ± s.e.m.

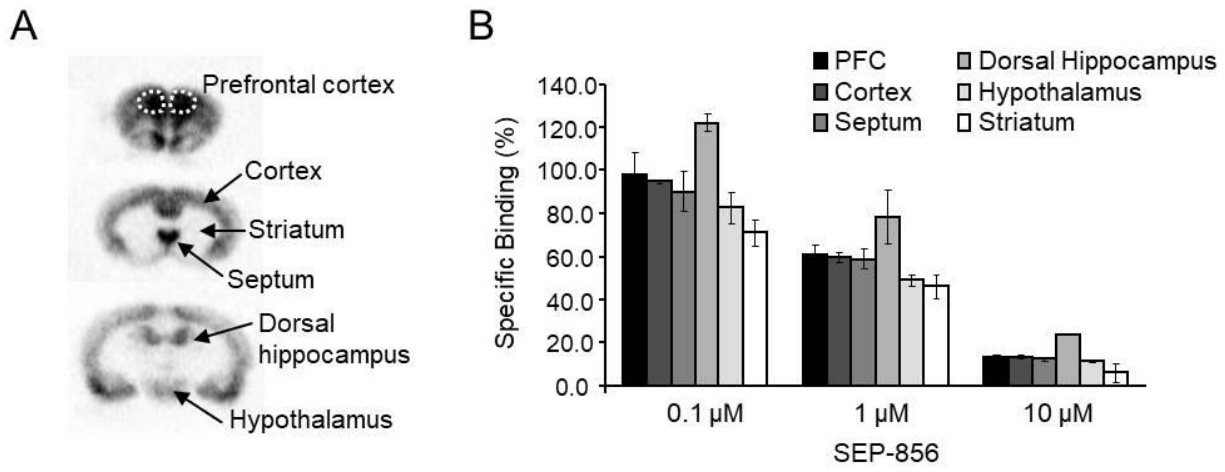

Supplemental Figure 5. SEP-856 binds to 5-HT_{1A} receptors in rat brain slices. (A) Autoradiographs of coronal brain sections depicting binding of the 5-HT_{1A} agonist [^{3}H]-8-OH-DPAT. SEP-856 displaced [^{3}H]-8-OH-DPAT in a concentration-dependent manner, in all brain regions tested. N = 4 brains, 2 sections/brain. Data are shown as mean ± s.e.m.

A

	Membrane potential (mV)			Membrane resistance (MΩ)		
	All DRN neurons	DPAT sensitive	DPAT insensitive	All DRN neurons	DPAT sensitive	DPAT insensitive
Mean	-46.1	-45.3	-47.2	849	809	898
SEM	1.0	1.4	1.4	61	62	115
n	29	16	13	29	16	13
p	-	-	0.36	-	-	0.48

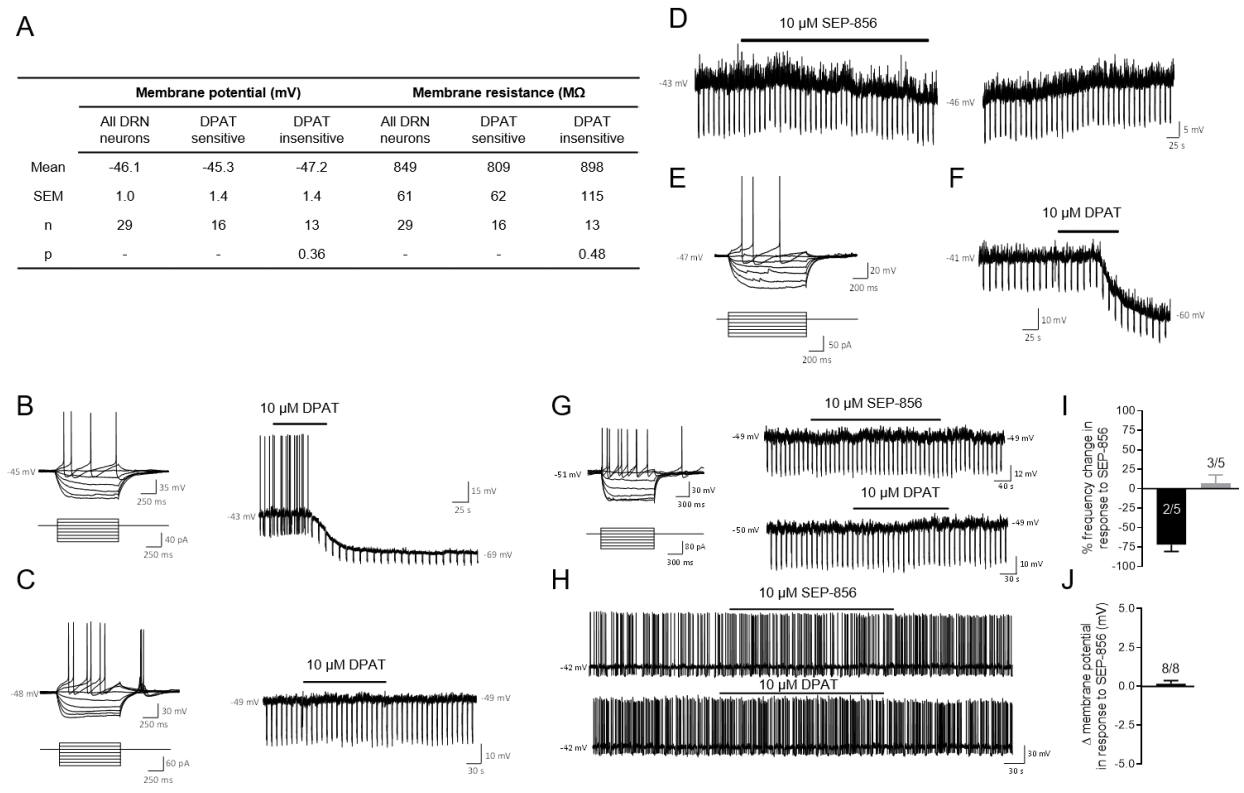

Supplemental Figure 6. Effects of SEP-856 on DRN firing. (A) Summary of the general properties of neurons recorded from the DRN. DRN neurons were classified based on their electrophysiological properties and response to administration of the 5-HT_{1A} receptor agonist [^{3}H]-8-OH-DPAT (DPAT). (B) Representative current/voltage relationship (left) of a DRN neuron in which DPAT induced a marked membrane hyperpolarization (right). (C) Representative current/voltage relationship (left) of a DRN neuron in which DPAT was without effect on membrane potential (right). Example of a current-clamp recording (D) and current/voltage relationship (E) of a quiescent, DPAT-sensitive DRN neuron in which SEP-856-induced membrane hyperpolarization. (F) Current-clamp recording of the DRN neuron shown in D and E during DPAT administration. SEP-856 had little effect in most DPAT-insensitive, quiescent (G) and spontaneously active (H) DRN neurons. (I, J) Quantifications of SEP-856 response (based on changes in membrane potential (mV) and/or firing rate (Hz) and expressed relative to baseline) in DPAT-insensitive DRN neurons. Solid bars indicate the timeframe of compound administration to the slice. Two-tailed t-test, * $p < 0.05$. Data are shown as mean ± s.e.m.

A

	Membrane potential (mV)	Membrane resistance (MΩ)	Firing rate (Hz)
Mean	-40.7	935	1.97
SEM	0.6	104	0.6
n	23	23	

B

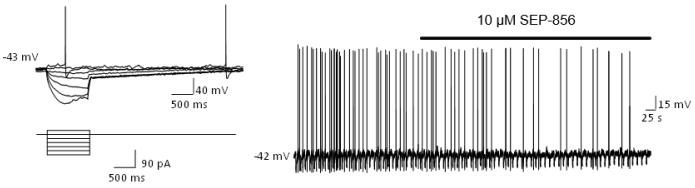

Supplemental Figure 7. Effects of SEP-856 on VTA firing. (A) Summary of the general properties of neurons recorded from the VTA. (B) Representative current/voltage relationship and current-clamp recording of a VTA neuron in which SEP-856 was without an effect. Solid bar indicates the timeframe of SEP-856 administration to the slice.

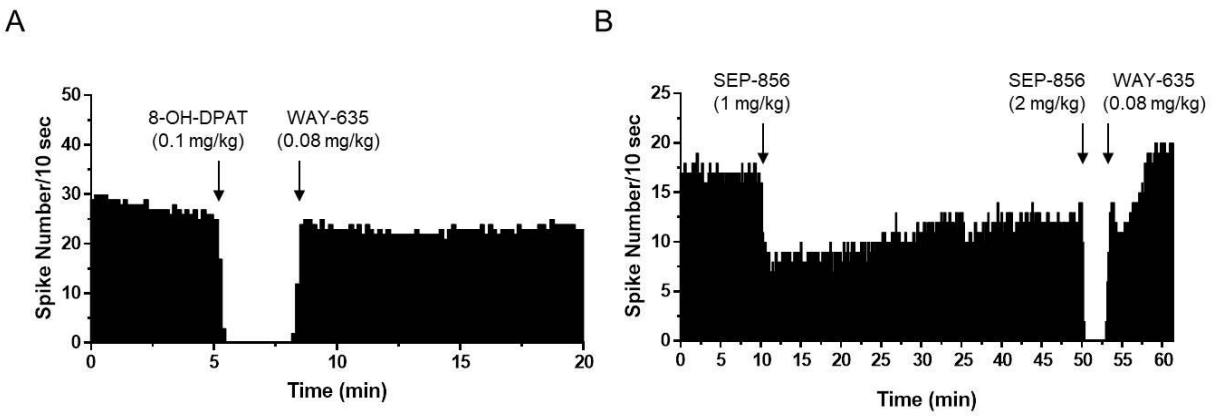

Supplemental Figure 8. SEP-856 inhibits firing of DRN in vivo through 5-HT_{1A}. (A) Single-unit discharges in DRN neurons were abolished following administration of the 5-HT_{1A} agonist 8-OH-DPAT (i.v.). The inhibition of firing was reversed by subsequent administration of the selective 5-HT_{1A} antagonist WAY-100635 (i.v., n = 1). (B) Rate histogram showing partial inhibitory effects of SEP-856 (1 mg/kg, i.v.) on single unit discharge of dorsal raphe nucleus. The inhibitory effect was time dependently reversed. Subsequent administration of SEP-856 at 2 mg/kg, i.v. resulted in a complete inhibition in discharge which was fully reversed by WAY-100635 (i.v., n = 1). Abbreviations: WAY-100635 (WAY-635).

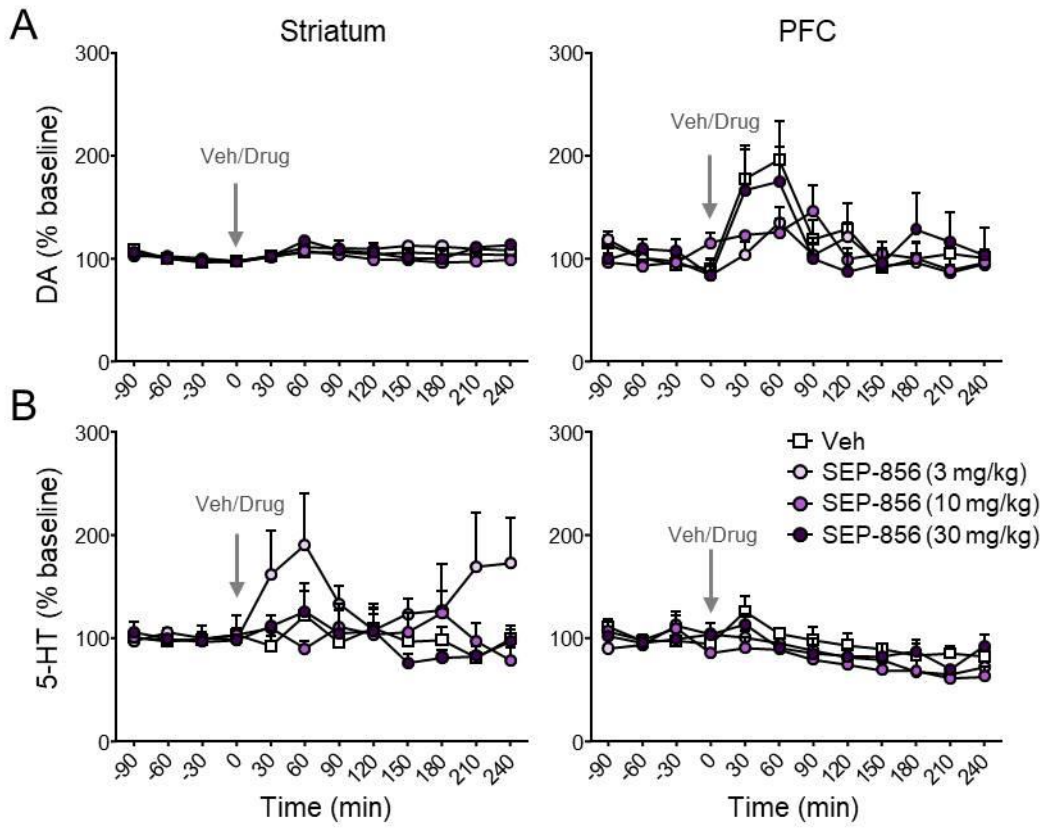

Supplemental Figure 9. Oral SEP-856 administration does not alter extracellular serotonin (5-HT) and dopamine (DA) levels in the striatum and prefrontal cortex (PFC) of male Sprague-Dawley rats. All treatments were administered at time = 0, following 90 minutes of baseline-sample collection. Monoamine levels are expressed as percent change from baseline. (A) SEP-856 (p.o.) at all doses tested did not affect extracellular DA levels in the striatum (two-way repeated measures ANOVA: treatment effect $F_{3,\ 509} = 1.3$, $p = 0.1$; time x treatment interaction $F_{(33,509)} = 1.34$, $p = 0.1$; n = 11-13/group) and PFC (two-way repeated measures ANOVA: treatment effect $F_{(3,\ 343)} = 0.85$, $p = 0.5$; time x treatment interaction $F_{(33,343)} = 1.4$, $p = 0.3$; n = 8-10/group). (B) Similarly, 5-HT release in the striatum and PFC was not affected by oral SEP-856 treatment compared to vehicle control (two-way repeated measures ANOVA: striatum - treatment effect $F_{(3,\ 240)} = 3.0$, $p = 0.05$; time x treatment interaction $F_{(33,240)} = 1.1$, $p = 0.35$; n = 5-9/group / PFC - treatment effect $F_{(3,\ 91)} = 3.5$, $p = 0.06$; time x treatment interaction $F_{(33,91)} = 0.9$, $p = 0.6$; 3-4/group). Data are shown as mean ± s.e.m.

Supplemental Tables

Supplemental Table 1. Cerep Bioprint Targets

A1	ETB	M2	5-HT6
A2A	GABAA	M3	5-HT7
A2B	GABAB(1b)	M4	σ
A3	glucagon	NK1	sst1
α1A	AMPA	NK2	sst4
α 1B	kainate	Y1	GR
α 2A	NMDA	N neuronal α-BGTX-insensitive (α4β2)	ERα
α 2B	glycine (strychnine-insensitive)	N muscle-type	AR
α 2C	CXCR4	δ2 (DOP)	TR (TH)
1	TNF–α	κ(KOP)	UT
β 2	CCR2	μ (MOP)	VPAC1 (VIP1)
β 3	H1	PPARγ	V1a
AT1	H2	PAF	V2
AT2	H3	PCP	Ca2+ channel (L, dihydropyridine site)
APJ (apelin)	H4	EP2	Ca2+ channel (L, diltiazem site) (benzothiazepines)
BZD	I1	FP	Ca2+ channel (L, verapamil site) (phenylalkylamine)
BB3	BLT1 (LTB4)	IP (PGI2)	Ca2+ channel (N)
B2	CysLT1 (LTD4)	LXRβ	SKCa channel
CB1	MCH1	PCP	Na+ channel (site 2)
CB2	MC1	5-HT1A	Cl- channel (GABA-gated)
CCK1 (CCKA)	MC3	5-HT1B	norepinephrine transporter
CCK2 (CCKB)	MC4	5-HT1D	dopamine transporter
CRF1	MT1 (ML1A)	5-HT2A	GABA transporter
D1	MT3 (ML2)	5-HT2B	5-HT transporter
D2S	MAO-A	5-HT2C	
D3	motilin	5-HT3	
ETA	M1	5-HT4e	

Supplemental Table 2. Cerep Enzyme Screen Targets

COX1	HIV-1 protease	p38α kinase
COX2	neutral endopeptidase	acetylcholinesterase
PDE2A	MMP-1	COMT
PDE3A	MMP-2	xanthine oxidase/ superoxide O2- scavenging
PDE4D	MMP-9	ATPase (Na+/K+)
PDE5 (non-selective)	Abl kinase	5-HT transporter
PDE6 (non-selective)	CDK2 (cycE)	p38α kinase
ACE	ERK2) (P42mapk)	acetylcholinesterase
ACE-2	FLT-1 kinase (VEGFR1)	COMT
BACE-1 (β-secretase)	Fyn kinase	xanthine oxidase/ superoxide O2- scavenging
caspase-3	IRK (InsR)	ATPase (Na+/K+)
caspase-9	Lyn A kinase (h)	5-HT transporter

Supplemental Table 3. Ricerca Receptor Screen Targets

Adenosine A1	Estrogen ERα	N-Formyl Peptide Receptor FPR1	Tachykinin NK3
Adenosine A2A	Estrogen ERβ	N-Formyl Peptide Receptor-Like FPRL1	Thyroid Hormone
Adenosine A3	GPR103	Neuromedin U NMU1	TRH
Adrenergic α1A	GABAA, Chloride Channel, TBOB	Neuromedin U NMU2	TGF-β
Adrenergic α1B	GABAA, Flunitrazepam, Central	Neuropeptide Y Y1	Transporter, Adenosine
Adrenergic α1D	GABAA, Muscimol,	Neuropeptide Y Y2	Transporter, Choline
Adrenergic α2A	GABAB1A	Neurotensin NT1	DAT
Adrenergic α2C	Gabapentin	Nicotinic Acetylcholine	Transporter, GABA
Adrenergic β1	Galanin GAL1	Nicotinic Acetylcholine α1, Bungarotoxin	Transporter, Monoamine
Adrenergic β2	Galanin GAL2	Nicotinic Acetylcholine α7, Bungarotoxin	NET
Adrenergic β3	Glucocorticoid 314541	NPBW2/GPR8	SERT
Adrenomedullin AM	Glutamate, AMPA	Opiate δ1 (OP1, DOP)	TNF, Non-Selective
Adrenomedullin AM2	Glutamate, Kainate	Opiate κ(OP2, KOP)	Urotensin II
Androgen	Glutamate, NMDA, Agonism	Opiate μ(OP3, MOP)	Vanilloid
Angiotensin AT2	Glutamate, NMDA, Glycine	Orphanin ORL1	VIP1
APJ	Glutamate, NMDA, Phencyclidine	Phorbol Ester	Vasopressin V1A
Atrial Natriuretic Factor (ANF)	Glutamate, NMDA, Polyamine	PDGF	Vasopressin V1B
Bombesin BB1	Glycine, Strychnine-Sensitive	Potassium Channel [KATP]	Vasopressin V2
Bombesin BB2	Growth Hormone Secretagogue (GHS)	Potassium Channel [SKCA]	Vitamin D3
Bombesin BB3	Growth Hormone Secretagogue (GHS)	Potassium Channel hERG	
Bradykinin B1	Histamine H1	Progesterone PR-B	
Bradykinin B2	Histamine H2	Prostanoid CRTH2	
Calcitonin	Histamine H3	Prostanoid DP	
Calcium Channel L-Type, Benzothiazepine	Histamine H4	Prostanoid EP2	
Calcium Channel L-Type, Dihydropyridine	Imidazoline I2	Prostanoid EP4	
Calcium Channel L-Type, Phenylalkylamine	Inositol Trisphosphate IP3	Purinergic P2X	
Calcium Channel N-Type	Interleukin IL-1	Purinergic P2Y 314632	
Cannabinoid CB1	Interleukin IL-6	Retinoid X RXRα	
Chemokine CCR1	Leukotriene, BLT (LTB4)	Ryanodine RyR3	
Chemokine CCR2B	Leukotriene, Cysteinyl CysLT1	5-HT1A	
Chemokine CCR4	Leukotriene, Cysteinyl CysLT2	5-HT2B	
Chemokine CCR5	Melanocortin MC1	5-HT2C	
Chemokine CX3CR1	Melanocortin MC3	5-HT3	
Chemokine CXCR2 (IL-8RB)	Melanocortin MC4	5-HT4	
Colchicine	Melanocortin MC5	5-HT5A	
Corticotropin Releasing Factor CRF1	Melatonin MT1	5-HT6	
Dopamine D1	Melatonin MT2	Sigma σ1	
Dopamine D2S	10 μM -1	Sigma σ2	
Dopamine D3	252200 Motilin	Somatostatin sst1	
Dopamine D4	Muscarinic M1	Somatostatin sst2	
Dopamine D5	Muscarinic M2	Somatostatin sst3	
Endothelin ETA	Muscarinic M3	Somatostatin	
Endothelin ETB	Muscarinic M4	Somatostatin sst5	
Epidermal Growth Factor (EGF)	Muscarinic M5	Tachykinin NK1	

Supplemental Table 4. Ricerca Enzyme Screen Targets

Catechol-O-Methyltransferase (COMT)	PDE2
Cholinesterase, Acetyl, ACES	PDE2A
Monoamine Oxidase MAO-A	PDE3
Monoamine Oxidase MAO-B	PDE3A
Nitric Oxide Synthase, Endothelial (eNOS)	PDE4
Nitric Oxide Synthase, Inducible (iNOS)	PDE4A1A
Nitric Oxide Synthase, Neuronal (nNOS)	PDE5
PDE1	PDE5A
PDE10A2	PDE6
PDE1A	

Supplemental Table 5. Pharmacokinetic properties of SEP-856.

Male ICR mice, Sprague-Dawley rats and rhesus macaques were dosed with SEP-856 by p.o. and/or i.v. administration. Parameters were derived from mean plasma or brain concentrations for n = 3 animals per dose route. Data are shown as mean or mean ± s.d.

Parameters	Mouse		Rat				Monkey	
	p.o.		i.v.	p.o.			i.v.	p.o.
	Plasma	Brain	Plasma	Plasma	Plasma	Brain	Plasma	
Dose (mg/kg)	10	10	5	5	10	10	5	5
AUC_{0-t} (ng*h/ml or ng*h/g)	7256	22442	3275 ± 567	1910 ± 144	4955	15102	6563 ± 2202	4708 ± 1694
$AUC_{0-\infty}$ (ng*h/ml or ng*h/g)	7273	22483	3306 ± 588	1930 ± 144	5352	16854	6677 ± 2173	3754
CL (L/h/kg)	-	-	1.54 ± 0.26	-	-	-	0.797 ± 0.223	-
V_{ss} (L/kg)	-	-	2.57 ± 0.1	-	-	-	3.59 ± 1.96	-
$MRT_{(0-\infty}$ (h)	1.95	2.06	1.41 ± 0.22	1.68 ± 0.03	3.01	3.54	3.33 ± 1.15	5.90
$t_{1/2}$ (h)	0.847	0.808	1.17 ± 0.16	1.24 ± 0.1	2.10	2.33	3.14 ± 1.26	3.03
t_{max} (h)	0.50	0.25	0.083	0.42 ± 0.14	0.25	0.25	0.083	6.00 ± 2.83
C_{max} (ng/ml or ng/g)	2854 ± 298	7972 ± 2908	2578 ± 110	1056 ± 173	1750 ± 369	3762 ± 1324	2191 ± 194	431 ± 104
Bioavailability (%)	-	-	58 – 120				71.4 ± 1.59	

Supplemental Table 6. Plasma and brain exposure to SEP-856 in mice and rats following single oral administration in different behavioral tests. Data are shown as mean ± s.d.

	SEP-856 (mg/kg)	Plasma (ng/ml)	Brain (ng/g)
Mouse PCP hyperactivity test[1]	0.3	4.8 (2.5)	42.6 (0.9)
	1	13.1 (7.3)	90.1 (42.6)
	3	85.6 (50.2)	367.3 (177.0)
Mouse PPI/startle[2]	0.3	5.6 ± 1.8	79.1 ± 22.1
	1	20.3 ± 3.7	255.8 ± 50.2
	3	181.3 ± 73.8	711.9 ± 89.7
	10	781.0 ± 169.4	2962.5 ± 373.3
	30	1965.0 ± 308.6	6368.8 ± 1560.9
Rat PCP social interaction test[3]	1	56.6 ± 10.5	380 ± 20.1
	3	112.4 ± 58.9	868.8 ± 458.4
	10	280.5 ± 173.2	1939.5 ± 1152.8

[1]Samples were collected from n = 4 mice per group at the end of behavioral testing, approximately 90 minutes after SEP-856 administration

[2] Samples were collected from n = 4 mice per treatment group at the end of behavioral testing, approximately 55 minutes after SEP-856 administration

[3] Samples were collected from n = 4 rats per treatment group at the end of behavioral testing, approximately 40 minutes after administration of SEP-856

Supplemental Table 7. SEP-856 occupancy of D_2 receptors measured with [^{3}H]-raclopride in rats.

In vivo occupancy of i.p. SEP-856 (10 mg/kg) at D_2 receptors was assessed in male Sprague-Dawley rats. [^{3}H]-raclopride was administered i.v. 30 minutes post SEP-856/vehicle dosing. Striatal and cerebellar (reference region) brain sections were assessed 30 min later using autoradiography. Data are shown as mean ± s.e.m; n = 6/group.

Treatment (i.p.)	Signal:Noise	% RO	Plasma (ng/ml)	Brain (ng/g)	B:P
Vehicle	5.7 ± 0.1	0 ± 8.5	NA	NA	NA
10 mg/kg	5.7 ± 0.3	12.6 ± 6.4	1321.7 ± 55.8	7858.3 ± 284.7	6.0 ± 0.2

Supplemental Table 8. In vivo occupancy of SEP-856 at D_2 receptors measured with [^{18}F]-fallypride-PET in nonhuman primates (*Papio anubis*).

[^{18}F]-fallypride binding potentials (BPND) were determined at baseline and following SEP-856 treatment using the non-invasive reference region model SRTM. BPND were subsequently used to estimate the receptor occupancy in several brain regions. SEP-856 was administered i.v. 30 minutes prior to [^{18}F]-fallypride injection. 3D PET scans were obtained continuously over 3 hours (T = 30-210 minutes). Data are shown as mean ± s.e.m.

Brain region	[^{18}F]-fallypride BP_{ND}		Receptor Occupancy (%)	Plasma (ng/ml)	
	Baseline	~ 7.25 mg/kg		60 min	180 min
Caudate	16.6 ± 5.7	15.2 ± 5.8	9.1 ± 3.3		
Putamen	20.3 ± 4.8	19.4 ± 5.9	6.2 ± 7.0	2850 ± 250	1765 ± 125
Globus Pallidus	8.3 ± 2.2	7.7 ± 2.7	9.6 ± 8.8		

References

Aghajanian GK, Wang RY, Baraban J, Serotonergic and non-serotonergic neurons of the dorsal raphe: reciprocal changes in firing induced by peripheral nerve stimulation Brain Res 1978 169-175.

Alexandrov V, Brunner D, Hanania T, and Leahy E (2015) High-throughput analysis of behavior for drug discovery. Eur J Pharmacol 750:82–89.

Clifford EM, Gartside SE, Umbers V, Cowen PJ, Hajós M, and Sharp T (1998) Electrophysiological and neurochemical evidence that pindolol has agonist properties at the 5-HT1A autoreceptor in vivo. Br J Pharmacol 124:206–212.

Hajós M, Allers KA, Jennings K, Sharp T, Charette G, Sík A, and Kocsis B (2007) Neurochemical identification of stereotypic burst-firing neurons in the rat dorsal raphe nucleus using juxtacellular labelling methods. Eur J Neurosci 25:119–126.

Martin LP, Jackson DM, Wallsten C, and Waszczak BL (1999) Electrophysiological comparison of 5-hydroxytryptamine1A receptor antagonists on dorsal raphe cell firing. J Pharmacol Exp Ther 288:820–826.

Roberds SL, Filippov I, Alexandrov V, Hanania T, and Brunner D (2011) Rapid, computer vision-enabled murine screening system identifies neuropharmacological potential of two new mechanisms. Front Neurosci 5:103.

Shao L, Campbell UC, Fang QK, Powell NA, Campbell JE, Jones PG, Hanania T, Alexandrov V, Morganstern I, Sabath E, et al. (2016) In vivo phenotypic drug discovery: applying a behavioral assay to the discovery and optimization of novel antipsychotic agents. MedChemComm 7:1093–1101.